https://doi.org/10.1093/plcell/koac107 THE PLANT CELL 2022: 34: 2688–2707

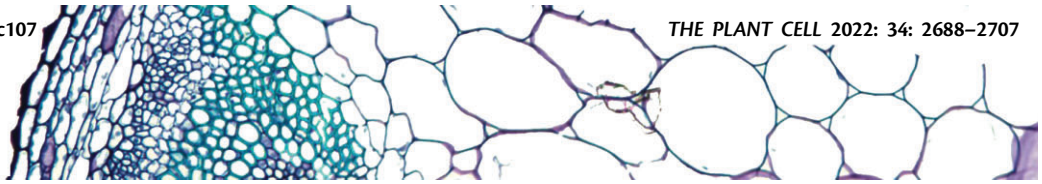

Research Article

AUXIN RESPONSE FACTOR7 integrates gibberellin and auxin signaling via interactions between DELLA and AUX/IAA proteins to regulate cambial activity in poplar

Jian Hu [1], Huili Su [1], Hui Cao [1], Hongbin Wei [1], Xiaokang Fu [1], Xuemei Jiang [1], Qin Song [1], Xinhua He [1,2,3], Changzheng Xu [1,*,†] and Keming Luo [1,4,*,†]

1 Chongqing Key Laboratory of Plant Resource Conservation and Germplasm Innovation, Integrative Science Center of Germplasm Creation in Western China (Chongqing) Science City, School of Life Sciences, Southwest University, Chongqing 400715, China
2 School of Biological Sciences, University of Western Australia, Perth, WA 6009, Australia
3 Department of Land, Air and Water Resources, University of California at Davis, Davis, California 95616, USA
4 Key Laboratory of Eco-environments of Three Gorges Reservoir Region, Ministry of Education, School of Life Sciences, Southwest University, Chongqing 400715, China

*Authors for correspondence: kemingl@swu.edu.cn (K.L); xucz@swu.edu.cn (C.X.).
†Senior authors

K.L., J.H., and C.X. designed the work and drafted the manuscript. J.H., H.S., H.C., and X.J. contributed new genetic materials. J.H., H.W., and X.F. analyzed the data. J.H. and Q.S. measured plant hormone levels. K.L. and C.X. revised the manuscript. X.H. provided valuable comments on the manuscript. All authors approved the final version of the manuscript for publication.
The author responsible for distribution of materials integral to the findings presented in this article in accordance with the policy described in the Instructions for Authors (https://academic.oup.com/plcell) is: Keming Luo (kemingl@swu.edu.cn).

Abstract

Cambial development in the stems of perennial woody species is rigorously regulated by phytohormones. Auxin and gibberellin (GA) play crucial roles in stimulating cambial activity in poplar (*Populus* spp.). In this study, we show that the DELLA protein REPRESSOR of *ga1-3* Like 1 (RGL1), AUXIN RESPONSE FACTOR 7 (ARF7), and Aux/INDOLE-3-ACETIC ACID 9 (IAA9) form a ternary complex that mediates crosstalk between the auxin and GA signaling pathways in poplar stems during cambial development. Biochemical analysis revealed that ARF7 physically interacts with RGL1 and IAA9 through distinct domains. The *arf7* loss-of-function mutant showed markedly attenuated responses to auxin and GA, whereas transgenic poplar plants overexpressing *ARF7* displayed strongly improved cambial activity. ARF7 directly binds to the promoter region of the cambial stem cell regulator *WOX4* to modulate its expression, thus integrating auxin and GA signaling to regulate cambial activity. Furthermore, the direct activation of *PIN-FORMED 1* expression by ARF7 in the RGL1–ARF7–IAA9 module increased GA-dependent cambial activity via polar auxin transport. Collectively, these findings reveal that the crosstalk between auxin and GA signaling mediated by the RGL1–ARF7–IAA9 module is crucial for the precise regulation of cambial development in poplar.

Received December 14, 2021. Accepted March 25, 2022. Advance access publication April 18, 2022

IN A NUTSHELL

Background: In trees, the vascular cambium is the population of stem cells that laterally divide and as a consequence, produce secondary xylem, which is commonly known as wood. The continuous activity of cambial cells determines the quantity of wood production. Multiple hormonal signals are known to rigorously regulate cambial activity. The exogenous application of auxin and gibberellin (GA) can promote cambium activity in poplar stems, and common transcriptome changes occur via treatment with these two phytohormones. However, how auxin and GA combinatorially regulate cambial activity in trees remains unknown.

Question: Does the crosstalk of auxin and GA signaling regulate cambial activity in trees, and if so, how does this occur? We addressed this issue by identifying the interactions of the key components of their signaling pathways in poplar.

Findings: The auxin response factor 7 (ARF7) acts as a core regulator of cambial activity to integrate both the auxin and GA pathways in poplar. ARF7 interacts with Aux/IAA and DELLA proteins at the same time. When auxin and GA are present, Aux/IAA and DELLA can be degraded, respectively, thereby releasing the ability of ARF7 to activate downstream gene expression. We found that *WOX4* (encoding a key cambial regulator) and *PIN1* (encoding an auxin efflux transporter) are directly targeted by ARF7. Therefore, the DELLA–ARF7–Aux/IAA complex regulates the crosstalk between auxin and GA, thereby regulating cambial activity in poplar, by targeting the key genes involved in cambial development.

Next steps: Scientists aim to genetically modify trees through molecular breeding to produce more wood and improve wood quality. Our work demonstrates that ARF7 acts as a molecular bridge linking auxin and GA signaling to regulate cambial activity in poplar, thereby providing a key target for the genetic engineering of trees for enhanced wood production.

Introduction

The populations of stem cells embedded in meristems survive throughout the lifetime of a plant and are essential for continuously supplying new cells. The apical meristems in the tips of shoots and roots drive primary/longitudinal growth, while the lateral meristem (vascular cambium) at the periphery of growth axes dominates secondary/radial growth (Greb and Lohmann, 2016). Following primary growth, undifferentiated procambial cells in primary vascular tissues and neighboring dedifferentiated parenchyma are unified to form a cylinder of cambium (Fischer et al., 2019). The cambium stem cells bilaterally produce secondary xylem and phloem via periclinal division, and their anticlinal division causes the cambial ring to enlarge to support an increase in girth (Campbell and Turner, 2017). In woody species, the perennial competence of the cambium determines the thickening of extended stems and the predominant deposition of secondary xylem, commonly known as wood, which is of great ecological and economic value.

Plant hormones play pivotal roles in cambial stem cell maintenance and activity (Bjorklund et al., 2007; Matsumoto-Kitano et al., 2008; Love et al., 2009; Sehr et al., 2010; Smetana et al., 2019). Early studies in sunflower (*Helianthus annuus*) showed that the application of exogenous auxin (indole-3-acetic acid [IAA]) to the apical bud suppressed meristematic activity, inducing cambial cell division and secondary xylem differentiation (Gouwentak, 1941). Similar results were obtained for many gymnosperm and angiosperm species, including *Arabidopsis thaliana* and *Populus* spp. (Sundberg et al., 2000; Little et al., 2002). For instance, secondary growth in stems was inhibited by removing the shoot apex (the main source of auxin) from *Populus* but was restored by supplying exogenous auxin (Bjorklund et al., 2007), suggesting that IAA produced by the apical shoot is required for cambial activity. Importantly, auxin displays distinct distribution profiles in different region of wood tissues, with the highest concentrations detected in the cambial zone and a gradual decrease with increasing differentiation of the derived tissues (Uggla et al., 1996; Tuominen et al., 1997; Uggla et al., 1998; Immanen et al., 2016). It is, therefore, assumed that the morphogen-like auxin gradients provides positional information for cambial derivates to achieve cell division and differentiation in a concentration-dependent manner (Uggla et al., 1998; Sundberg et al., 2000).

Auxin regulates vascular development through its signaling pathway, which includes the auxin receptor TRANSPORT INHIBITOR RESPONSE 1, auxin/IAA-inducible Aux/IAA proteins, and AUXIN RESPONSE FACTOR (ARF) transcription factors (Burroughs et al., 2007; Guilfoyle and Hagen, 2007; Dinesh et al., 2016). Overexpression of *IAA3m*, encoding a stabilized form of IAA3 that perturbs auxin signaling, repressed the periclinal division of cambial cells but promoted anticlinal cell division in *Populus tremula* × *Populus tremuloides* (Nilsson et al., 2008). The poplar *PIN-FORMED* genes *PttPIN1* and *PttPIN12*, which are expressed in cambial meristem and extended xylem derivatives, play key roles in polar auxin transport in stems (Schrader et al., 2003). ARF5/MONOPTEROS (MP) is activated by auxin signals and increases the number of vascular initial cells by positively regulating *PIN1* expression in procambial stem

cells (Wenzel et al., 2007; Smetana et al., 2019; Zhang et al., 2019). Furthermore, during the secondary growth of Arabidopsis, ARF5 modulates vascular proliferation during early development but suppresses vascular expansion during late development (Brackmann et al., 2018; Han et al., 2018). Other ARFs, including ARF3 and ARF4, combinatorially regulate cambial activity (Brackmann et al., 2018). Although these findings suggest that auxin signaling is required for regulating secondary vascular development, the detailed mechanism is complex due to the crosstalk between auxin and other hormone signaling pathways and therefore remains largely unknown.

The physiological roles of gibberellin (GA) in cambial development have been intensively studied. In *Populus*, bioactive GA peaks are detected in developing xylem (Immanen et al., 2016). Constitutive or xylem-specific expression of *PdGA20ox1* from the pine *Pinus densiflora* encoding GA20 oxidase, a key enzyme that catalyzes the production of bioactive GA forms from GA_{12}, increased xylem width and cell number in transgenic hybrid poplar (Jeon et al., 2016). GA signaling is crucial for the formation of xylem fibers and for stimulating xylem expansion in hypocotyls (Chaffey et al., 2002; Ragni et al., 2011; Ben-Targem et al., 2021). However, the application of exogenous GA to decapitated stems of various plant species activated the division and expansion of cells in the cambial zone, but not xylem differentiation (Wareing, 1964; Little and Savidge, 1987). Increased GA levels improved cambial growth in transgenic poplar (Israelsson et al., 2005), suggesting that GA also plays a vital role in regulating vascular cambial activity. Similarly, overexpressing *GA20ox* and the GA receptor gene *GID1* in poplar resulted in enhanced cambial proliferation and secondary growth (Mauriat and Moritz, 2009), whereas mutants with defects in GA biosynthesis showed reduced cambial activity (Ragni et al., 2011).

Increasing evidence indicates that WUSCHEL-RELATED HOMEOBOX4 (WOX4) plays a central role in the network regulating cambial activity, as it integrates auxin, TRACHEARY ELEMENT DIFFERENTIATION INHIBITORY FACTOR/PHLOEM INTERCALATED WITH XYLEM (PXY), and ethylene signaling to promote cambium cell division in trees and herbaceous species (Hirakawa et al., 2010; Suer et al., 2011; Etchells et al., 2013; Zhang et al., 2019). *WOX4* expression was activated by exogenous auxin (IAA) treatment in Arabidopsis inflorescence stems (Suer et al., 2011; Kucukoglu et al., 2017). Conversely, cambium cell proliferation was reduced and secondary growth was severely inhibited in *WOX4*-RNAi transgenic *Populous* stems, indicating that WOX4 is required for auxin-dependent modulation of cambial activity (Kucukoglu et al., 2017). Auxin-induced *ARF5/MP* activity directly reduced the expression of *WOX4*. ARF5/MP functions in vascular stem cell maintenance in Arabidopsis inflorescence stems in a cell-autonomous manner (Brackmann et al., 2018; Smetana et al., 2019).

Auxin and GA signals have synergistic effects on cambial development during the secondary growth of vascular tissue (Bjorklund et al., 2007). GA treatment improves auxin accumulation in poplar stems by stimulating polar auxin transport. Transcriptome analysis showed that most genes affected by increasing auxin levels are also induced by increasing GA levels (Bjorklund et al., 2007), suggesting that auxin and GA regulate cambial activity through a common downstream signaling pathway. In general, the GA signaling pathway is negatively modulated by DELLA proteins (Peng et al., 1997; Sun, 2010; Hu et al., 2018). In Arabidopsis, GA molecules drive DELLA degradation and promote xylem expansion (Ragni et al., 2011). DELLA proteins physically interact with many transcription factors, including ERFs, MYBs, NACs, and WRKYs (Marin-de la Rosa et al., 2014; Hu et al., 2018; Ben-Targem et al., 2021). ARF6 and ARF8 physically interact with DELLAs to specifically inhibit phloem proliferation and improve cambium senescence (Ben-Targem et al., 2021). However, how the interactions between DELLAs and ARFs contribute to the GA-auxin-induced regulation of cambium activity in trees has been unclear.

Here, to examine how the crosstalk between GA and auxin signaling regulates cambial activity in poplar, we modulated the endogenous levels and signaling pathways of these phytohormones. We found that the RGL1–ARF7–IAA9 module plays a central role in the crosstalk between GA and auxin signaling in cambial cells. Our findings provide insights into the role of the auxin and GA regulatory network in cambial activity during wood formation in poplar stems.

Results

Crosstalk between GA and auxin signaling regulates cambial activity

To confirm that auxin and GA signals have synergistic effects on cambial development during the secondary growth of vascular tissue in popular, we examined cambium phenotypes after the application of the auxin IAA and GA. Our experiments confirmed the synergistic effects of these phytohormones on this process (Supplemental Figure S1, A–D). To further explore the effects of these phytohormones, we modulated endogenous GA contents in poplar stems. We cloned the genes encoding GA 3-oxidase (GA3ox), a key enzyme for the synthesis of bioactive GAs, and GA 2-oxidase (GA2ox), an enzyme that deactivates endogenous GAs, from *Populus tomentosa* under the control of the *LMX5* promoter, as this gene is mainly expressed in developing xylem and cambial cells (Love et al., 2009). Bioactive GA levels significantly increased in $LMX5_{pro}$:*GA3ox* transgenic poplar plants, which exhibited increased plant height and stem diameter compared to wild-type (WT) plants. The opposite phenotype was found in $LMX5_{pro}$:*GA2ox* transgenic poplar, in which GA levels were reduced by *GA2ox* expression (Supplemental Figure S2, A–F). The changes in endogenous GA levels severely affected wood yields, as indicated by the *GA3ox*-/*GA2ox*-induced changes in xylem percentage due to *GA3ox* or *GA2ox* expression in transgenic stems (Supplemental Figure S3, A and B). Consistently, more xylem cell layers were observed in

LMX5$_{pro}$:*GA3ox* transgenic plants compared to WT, whereas fewer xylem cell layers were observed in *LMX5*$_{pro}$:*GA2ox* transgenic lines (Supplemental Figure S3, C and D).

To investigate the cambial activity that was modified by altered GA levels, we measured the width and number of cell layers in the cambial zones of the transgenic lines (Supplemental Figure S4A). More cells were present in the cambial cell files in the *LMX5*$_{pro}$:*GA3ox* lines than WT, whereas fewer of these cells were found in the *LMX5*$_{pro}$:*GA2ox* lines (Supplemental Figure S4, B and C), revealing the effect of GA levels on periclinal cell division. Moreover, the frequency of anticlinal cell divisions in each cambial cell layer was higher in the *LMX5*$_{pro}$:*GA3ox* lines than WT (Supplemental Figure S4D). In contrast, the reduced GA levels in the *LMX5*$_{pro}$:*GA2ox* lines not only restricted the frequency of anticlinal cell division, but they also modified its spatial pattern in the radial direction (Supplemental Figure S4D). These results indicate that endogenous GA accumulation plays an important role in regulating cambial activity.

We investigated whether the effects of local GA signaling on cambial activity depend on DELLAs, which function as negative regulators of GA signaling (Peng et al., 1997; Sun, 2010). Two homologous pairs of *DELLA* genes were identified in the *P. trichocarpa* genome database Phytozome (https://phytozome-next.jgi.doe.gov) (Supplemental Figure S5A). Among these genes, *RGL1* exhibits the highest transcript abundance in the cambial zone (Supplemental Figure S5B). Despite its strong enrichment in phloem, Yellow Fluorescent Protein (YFP)-labeled RGL1 driven by its native promoter was detected in cambial cells (Supplemental Figure S5, C and D). RGL1 harbors the canonical GRAS and DELLA domains (Supplemental Figure S6A) and is destabilized by GA treatment (Supplemental Figure S6, B–D). A deletion of 17 amino acids covering the DELLA motif (ΔRGL1) drastically impeded the GA-sensitive protein turnover of RGL1 (Supplemental Figure S6, A–D), resembling its counterpart in Arabidopsis (Dill et al., 2001). We introduced the mutated degradation-resistant version of *RGL1* (Δ*RGL1*) under the control of the cambium-specific *WOX4a* promoter (Kucukoglu et al., 2017) into poplar plants. The wood formation phenotypes of the *WOX4a*$_{pro}$:Δ*RGL1* transgenic lines were similar to those of the *LMX5*$_{pro}$:*GA2ox* lines (Supplemental Figure S7, A–D). Moreover, the cambium growth and division phenotypes resulting from the cambium-specific expression of Δ*RGL1* almost completely mimicked those of the GA-deficient lines (Supplemental Figure S8, A–D). Therefore, the effect of GA on cambial activity principally depends on its local signaling pathway in the cambial zone.

We then addressed the effect of the crosstalk between auxin and GA signaling on cambial development. Compared to mock treatment, exogenous IAA treatment strongly increased the cell division activity and modified the spatial pattern of anticlinal cell division in the cambium of plants in the *LMX5*$_{pro}$:*GA2ox* background (Figure 1, A and B; Supplemental Figure S9, A and B). To test the effect of auxin signaling on wood formation at the site of GA accumulation, we expressed *IAA9m*, encoding an auxin-resistant form of poplar IAA9 (a crucial repressor of auxin signaling; Xu et al., 2019), under the control of the *WOX4a* promoter in plants over-accumulating GA (Supplemental Figure S10, A and B). Xylem development was significantly suppressed in these transgenic plants compared to WT (Supplemental Figure S10, C and D). Notably, the cambium-specific inhibition of auxin signaling via *IAA9m* expression compromised the GA-enhanced periclinal and anticlinal division of cambial cells (Figure 1, C and D; Supplemental Figure S11, A and B). These results suggest that crosstalk between GA and auxin signaling occurs during cambial development in poplar.

We also tested the effects of GA and auxin treatment on *WOX4a*$_{pro}$:Δ*RGL1* transgenic plants, in which GA signaling was locally blocked in the cambium. The application of exogenous GA and IAA together strongly stimulated cambial growth and division in WT (Figure 1, E and F; Supplemental Figure S12, A and B), in accordance with a previous report (Bjorklund et al., 2007). Treatment with exogenous GA alone did not modify the cambial phenotypes of *WOX4a*$_{pro}$:Δ*RGL* (Figure 1, E and F; Supplemental Figure S12, A and B), validating the local GA signaling-dependent regulation of cambial activity. In contrast, although exogenous IAA induced cambium growth in *WOX4a*$_{pro}$:Δ*RGL* transgenic plants, this effect was markedly attenuated compared to WT (Figure 1F; Supplemental Figure S12A). Similar results were obtained when we measured the frequency of periclinal and anticlinal divisions in the cambial zone (Figure 1F; Supplemental Figure S12, A and B). Taken together, these results suggest that GA and auxin signaling combinatorially regulate cambial activity.

DELLA proteins physically interact with ARF7

DELLAs play crucial roles in mediating crosstalk between the GA and auxin signaling pathways through their physical interactions with various ARF transcription factors that trigger auxin-inducible gene expression in Arabidopsis (Oh et al., 2014; Ben-Targem et al., 2021). We reasoned that DELLAs and the ARF/IAA complex might mediate crosstalk between GA and auxin signaling to regulate cambial development in poplar. Phylogenetic analysis revealed that the ARF proteins in poplar belong to four subclades corresponding to paralogs of Arabidopsis ARF5, ARF6, ARF7, and ARF8 (Supplemental Figure S13A). We chose a representative member from each ARF subclade to examine its interaction with RGA1 and RGL1 in yeast two-hybrid (Y2H) assays. The truncated forms of *RGA1* and *RGL1* encoding the GRAS domain located at the C-terminus were fused to the BD vector (RGA1-c and RGL1-c) to prevent the self-activation activity of the full-length proteins, as reported in Arabidopsis (An et al., 2012). These DELLAs indeed interacted with ARF6, ARF7, and ARF8 in this assay (Supplemental Figure S13B). We then examined the expression patterns of the genes encoding DELLA-interacting ARF proteins in poplar stems during secondary growth. We first evaluated the expression levels of these *ARF* genes in the third to ninth internodes of

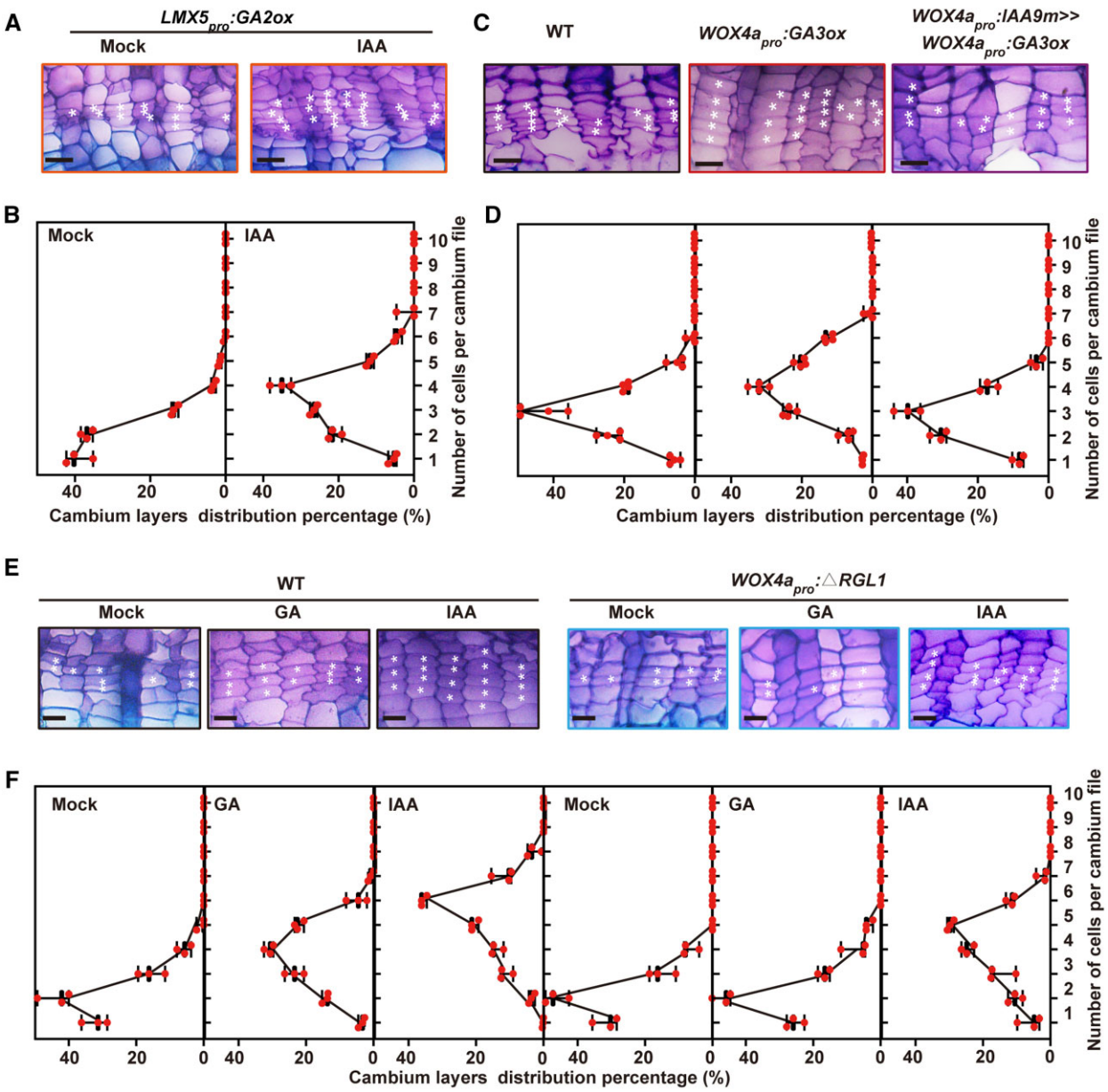

Figure 1 Cambial activity in poplar depends on crosstalk between local GA and auxin signaling pathways. A, C, and E, Toluidine blue-stained anatomical sections of the eighth internodes of *LMX5*$_{pro}$*:GA2ox* transgenic lines after 3 weeks of mock or IAA treatment (A); 2-month-old WT, *WOX4a*$_{pro}$*:GA3ox*, and *WOX4a*$_{pro}$*:IAA9m*≫*WOX4a*$_{pro}$*:GA3ox* lines (C), and WT and *WOX4a*$_{pro}$*:ΔRGL1* lines under mock, GA, and IAA treatment (E). White asterisks indicate the cambium cell layer. Bars, 20 μm. B, D, and F, Frequency distribution of cell numbers in the cambium of the eighth internodes of *LMX5*$_{pro}$*:GA2ox* transgenic lines under mock (left) and IAA (right panel) treatment (B), WT (left), *WOX4a*$_{pro}$*:GA3ox* (middle), and *WOX4a*$_{pro}$*:IAA9m*≫*WOX4a*$_{pro}$*:GA3ox* (right) lines (D), and WT (first three parts) and *WOX4a*$_{pro}$*:ΔRGL1* (last three parts) lines under mock, GA, and IAA treatment (F). For (B), (D), and (F), $n = 3$.

the stem. Only *ARF7.2* and *ARF7.3* showed obviously increasing transcript abundance along the internodes downward (Supplemental Figure S13C), pointing to their roles in the secondary growth of vascular tissue in poplar stems. We selected ARF7.2, a member of this homolog pair, for further analysis of DELLA–ARF protein interactions.

As observed in the preliminary Y2H screening described above, the interactions between ARF7.2 and the truncated forms of both RGA1 and RGL1 were confirmed in yeast cells (Figure 2A). We tested the interactions of RGA1 and RGL1 with ARF7.2 in bimolecular fluorescence complementation (BiFC) assays. Strong fluorescent signals overlapping with DAPI staining were observed when RGL1 and ARF7.2 labeled by N- or C-terminal YFP were transiently co-transfected into leaf epidermal cells of *Nicotiana benthamiana* (Figure 2B). Their physical interactions in plant cells were also validated by co-immunoprecipitation (Co-IP) experiments (Figure 2C). Additionally, RNA in situ hybridization revealed the presence of both *ARF7.2* and *RGL1* transcripts in the cambial zone of the stem (Figure 2, D–E). Fluorescence-labeled RGL1 was

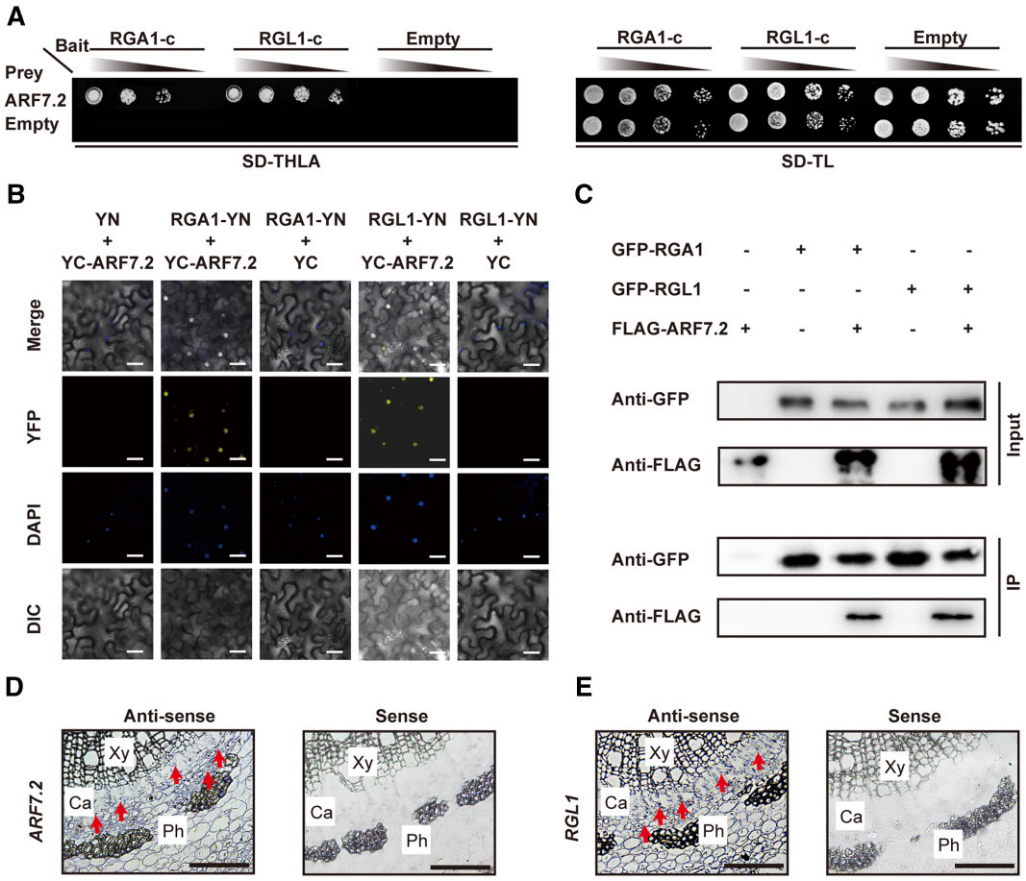

Figure 2 ARF7 and DELLAs interact and are co-expressed in the cambium. A, Protein interactions between ARF7.2 and RGA/RGL1, as determined by Y2H assays. The C-termini of both RGA and RGL1 were altered to eliminate their capacity for self-activation. Yeast cells cultivated on medium without tryptophan, histidine, leucine, and adenine (SD-THLA) were used as a positive control. B, Protein interactions between ARF7.2 and RGA/RGL1, as determined by BiFC assays. Full-length ARF7.2 and RGA/RGL1 were fused to the split C- or N-terminal fragment of yellow fluorescent protein (cYFP/YC or nYFP/YN). *Nicotiana benthamiana* leaf epidermal cells co-transformed with each pair of YC-ARF7.2 and DELLA-YNs were photographed in dark field for yellow fluorescence and DAPI staining and under bright light to visualize cell morphology; merged images are also shown. Bar, 50 μm. C, Validation of the physical association between ARF7.2 and DELLAs in vivo by Co-IP assays. Green Fluorescent Protein (GFP)-DELLAs were transiently expressed with FLAG-ARF7.2 in *N. benthamiana*. Protein extracts were immunoprecipitated with anti-green fluorescent protein (anti-GFP) antibody and immunoblotted using anti-GFP and anti-Flag antibodies. D and E, In situ hybridization to examine the expression of *ARF7.2* and *RGL1* in poplar stems. Cross-sections of the seventh internodes of 2-month-old *P. tomentosa* cultivated in soil were hybridized with antisense and sense probes of *ARF7.2* and *RGL1*, respectively. Red arrows indicate in situ hybridization signals. Ca, cambium; Ph, phloem; Xy, xylem. Bar, 100 μm.

also detected in the cambial cells (Supplemental Figure S5, C–D). Thus, these results confirm the physical interaction between RGL1 and ARF7.2.

RGL1, ARF7, and IAA9 form a ternary complex

Poplar ARF7.2 exhibits the typical structure of ARF proteins, which are characterized by a modular structure containing an N-terminal B3 motif, a middle region (MR), and a C-terminal PB1 domain (Guilfoyle and Hagen, 2007). To assess which domain of ARF7.2 interacts with RGL1, we constructed a series of ARF7.2 truncation constructs, as shown in Figure 3A. Truncated proteins with the MR domain (ARF7.2Δ and ARF7.2-MR) interacted with RGL1 as strongly as full-length ARF7.2 in an Y2H assay (Figure 3B). Yeast self-activation analysis showed that the transcriptional activation activity of ARF7.2 depends on the MR domain (Supplemental Figure S14A). Interestingly, the MR domain of ARF5.1 did not interact with RGL1 (Supplemental Figure S13B).

To verify the role of the MR domain in the DELLA–ARF interaction, we swapped the MR domains of ARF5.1 and ARF7.2 (Figure 3C). The replacement of MR ($ARF7.2^{757}$) abolished the physical interaction of ARF7.2 with RGL1 (Figure 3D), but it did not affect the activation ability of ARF7.2 (Supplemental Figure S14A). On the contrary, when the MR domain of ARF5.1 was substituted with that of ARF7.2 ($ARF5.1^{575}$), ARF5.1 acquired the ability to interact with DELLA (Figure 3C), indicating that the MR domain of ARF7.2 is responsible for the interaction with DELLA. ARFs are known to form heterodimers with Aux/IAA proteins via their C-terminal PB1 domains (Vernoux et al., 2011). Our Y2H assays confirmed that ARF7.2 strongly interacts with IAA9 (Supplemental Figure S14B).

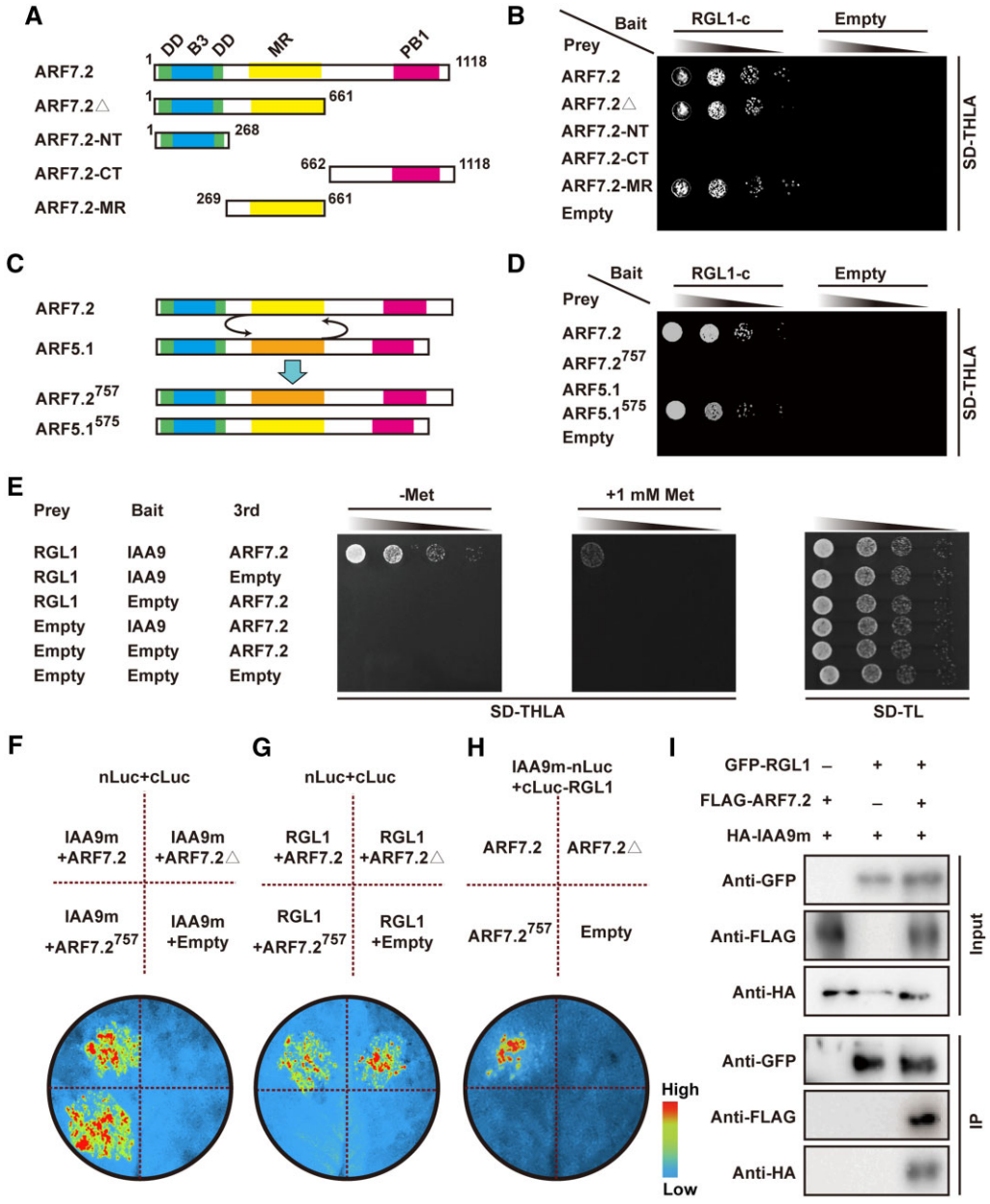

Figure 3 DELLA and Auxin/IAA proteins interact with ARF7 to form a ternary complex. A and C, Diagrams of the full-length and truncated forms of ARF7.2 (A), and swapping of the MR domains between ARF5.1 and ARF7.2 (C). DD, dimerization domain; DBD, DNA-binding domain; PB1, Auxin/IAA binding domain. Numbers refer to amino acids. B and D, RGL1 binds to the MR domain of ARF7.2 in Y2H assays. The ability of yeast cells to grow on medium without tryptophan, histidine, leucine, and adenine (SD-THLA) was scored as a positive interaction. SD-TL: synthetic medium lacking tryptophan and leucine. E, Experimental validation of the ARF7.2-directed association between RGL1 and IAA9 by Y3H assays. An undecorated ARF7.2 protein was expressed under the control of the *MET25* promoter (*MET25*$_{pro}$:*ARF7.2*) in *pBridge*, while *pBridge* plasmids lacking the CDS of ARF7.2 were used as negative controls (empty). The *MET25* promoter is repressed in the presence of 1-mM methionine and expressed in the absence of methionine. F and G, Detecting the interaction domains of ARF7.2 with IAA9 (F) and RGL1 (G) in *N. benthamiana* leaf epidermal cells by LCI assays. The full-length, substituted, and truncated forms of ARF7.2 were fused to cLUC to identify the interacting domain. H, Detection of the ARF7.2-directed association between RGL1 and IAA9 in *N. benthamiana* leaf epidermal cells via LCI assays. The full-length, substituted, and truncated forms of ARF7.2 were used to examine the ARF7.2-directed association. IAA9m, an auxin-resistant form of IAA9, was used to prevent the auxin-promoted instability of IAA9 proteins. Empty vector was used as a negative control. The color-coded regions in (F), (G), and (H) indicate the intensity of luciferase activity. I, Validation of the IAA9–ARF7.2–RGL1 ternary complex via Co-IP assays. Constructs harboring *GFP-RGL1*, *HA-IAA9m*, and *FLAG-ARF7.2* were co-transfected into *N. benthamiana*. Total protein extracts were immunoprecipitated with anti-green fluorescent protein (anti-GFP) antibody and immunoblotted using anti-GFP, anti-HA, and anti-Flag antibodies.

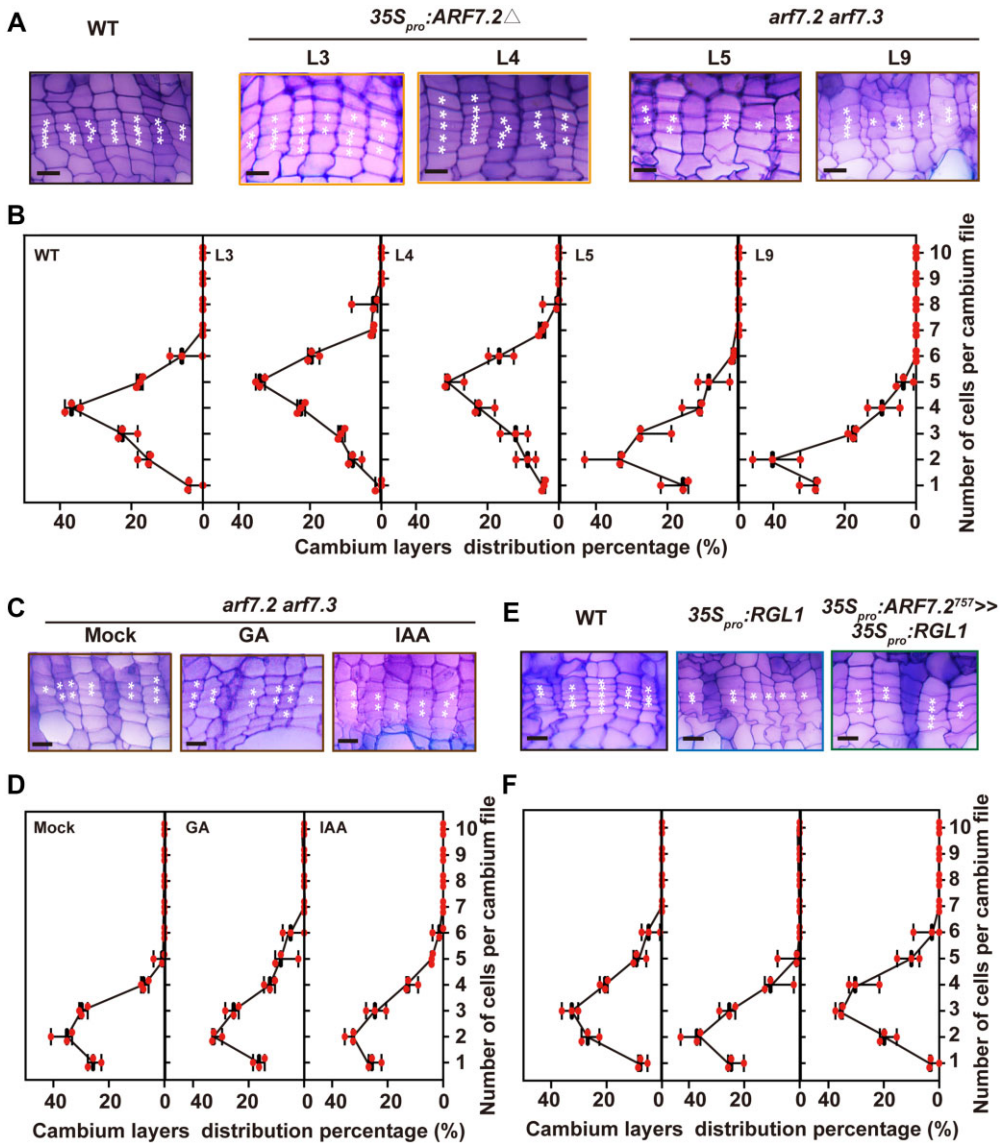

Figure 4 ARF7 integrates auxin and GA signaling to regulate cambial activity. A, C, and E, Toluidine blue-stained anatomical sections of the eighth internodes of WT, 35S$_{pro}$:*ARF7.2*Δ and *Cas9-ARF7.2/7.3* lines (A), *Cas9-ARF7.2/7.3* transgenic lines under mock, GA, and IAA treatment (C), and WT, 35S$_{pro}$:*RGL1*, and 35S$_{pro}$:*ARF7.2*^{757}≫35S$_{pro}$:*RGL1* lines (E). White asterisks indicate the cambium cell layers. Bars, 20 μm. B, D, and F Frequency distributions of cell numbers in the cambium region of the eighth internode of WT (left), 35S$_{pro}$:*ARF7.2*Δ (second and third parts) and *arf7.2 arf7.3* (fourth and fifth parts) lines (B), *arf7.2 arf7.3* lines under mock, GA, and IAA treatment (C), and WT (left), 35S$_{pro}$:*RGL1* (middle), and 35S$_{pro}$:*ARF7.2*^{757}≫35S$_{pro}$:*RGL1* (right) lines (F). For (B), (D), and (F), $n = 3$.

Given that the different domains of ARF7.2 are responsible for its interaction with DELLA or Aux/IAA proteins, we hypothesized that these proteins are capable of forming a ternary complex. To verify this idea, we performed yeast three-hybrid (Y3H) assays. Positive colonies co-transformed with both RGL1 and IAA9 were detected only in the presence of ARF7.2 (Figure 3E), suggesting that ARF7.2 might act as a molecular bridge to form a complex with RGL1 and IAA9. To further validate the molecular interactions among these proteins, we conducted firefly luciferase complementation imaging (LCI) assays in *N. benthamiana* leaves. As expected, both IAA9 and RGL1 strongly interacted with ARF7.2 in the LCI system (Figure 3, F–G). Luminescence emitted by the IAA9–RGL1 combination was detected when full-length ARF7.2 was present, while the luminescent signals were abolished due to the lack of the PB1 domain (ARF7.2Δ) or the MR substitution (ARF7.2^{757}) (Figure 3H). Therefore, these two domains mediate the interactions of ARF7.2 with IAA9 or RGL1. These results were confirmed by Co-IP assays (Figure 3I). Altogether, the in vitro and in vivo evidence shows that ARF7 directly interacts with RGL1 and IAA9 to form a ternary complex.

ARF7 integrates the crosstalk of GA and auxin signaling to regulate cambial activity

To explore the genetic regulation of the secondary growth of poplar stems, we generated *ARF7.2*-overexpression and -CRISPR/Cas9-knockout (*arf7.2 arf7.3*) lines (Supplemental

Figure S15, A and B). Due to the possibly functional redundancy of the paralogs *ARF7.2* and *ARF7.3*, we designed four sgRNA-targeted sites in the highly conserved regions of their cDNAs to create double knockout mutants. Two transgenic lines generated by the CRISPR/Cas9 system harbored fragment deletions in *ARF7.2* and *ARF7.3* (Supplemental Figure S15, C and D). As shown by quantifying the percentage of xylem in stems, secondary xylem differentiation increased in the *ARF7.2*-overexpressing lines but deceased in the *arf7.2 arf7.3* lines (Supplemental Figure S16, A and B). We investigated the cambial phenotypes of these transgenic lines and found that *ARF7.2*Δ overexpression enhanced the number of cambial layers and the division frequency of cambial cells, whereas *arf7.2 arf7.3* suppressed cambial division activity (Figure 4, A and B; Supplemental Figure S16, C and D). These opposite phenotypes suggest that ARF7 positively regulates cambial activity.

We treated the *arf7.2 arf7.3* plants with exogenous GA and IAA. These phytohormones had little effect on cambial cell division or secondary growth (Figure 4, C and D; Supplemental Figure S17, A and B). We introduced *ARF7.2*^{757}, encoding a chimeric ARF7 protein lacking binding activity to DELLAs, into *RGL1*-overexpressing plants. The inhibited wood development was complemented by the transgene (Supplemental Figure S18, A–D). The introduction of *ARF7.2*^{757} not only largely restored the cambial cell layers, but it also promoted cambium division activity (Figure 4, E and F, Supplemental Figure S19, A and B). These results provide genetic evidence for the role of ARF7 in mediating the regulatory effects of GA and auxin signaling on cambial activity.

GA and auxin signaling synergically regulate *WOX4* expression in the cambium

Previous microarray-based global transcriptome analyses of poplar stems revealed that the application of GA and auxin induce similar downstream signaling pathways (Bjorklund et al., 2007). To identify the target genes of the GA and auxin signaling pathways involved in regulating cambial development, we analyzed this transcriptome data set and identified 398 genes that were more highly induced by the simultaneous application of these phytohormones than the application of either hormone alone (Supplemental Figure S20A). Among these, 86 genes belonged to the cluster of cambium-specific genes identified in the AspWood database (Sundell et al., 2017). Gene functional annotation revealed that four of these genes encode transcription factors, including *WOX4a/b*, *GATA transcription factor 8* (*GATA8*), and *TSO1-like transcription factor 1* (*SOL1*) (Supplemental Figure S20A). As revealed by the expression data from the AspWood database (Sundell et al., 2017), these four genes exhibited high transcript abundance in the cambial zone (Supplemental Figure S20B). We measured the expression levels of these transcription factor genes in *WOX4a*$_{pro}$:Δ*RGL1* transgenic plants in response to GA and auxin by RT-qPCR. *WOX4a/b* expression levels were not affected by GA treatment (Supplemental Figure S20C), as GA signaling was specifically blocked in the cambium in these plants. Similarly, the auxin-induced expression of these genes was dramatically impaired in *WOX4a*$_{pro}$:Δ*RGL1* plants. Compared to WT, the auxin-induced expression decreased from 3.0- to 1.2-fold for *WOX4a* and 2.8- to 1.6-fold for *WOX4b* (Supplemental Figure S20C). In contrast, the cambium-specific expression of Δ*RGL1* failed to block the GA response of *GATA8* but repressed auxin-induced *SOL1* expression (Supplemental Figure S20C).

Due to the key role of *WOX4* in maintaining cambium division (Kucukoglu et al., 2017), we reasoned that *WOX4a/b* might function as the downstream targets of the GA and auxin pathways to regulate cambial development. To verify this notion, we measured the expression levels of *WOX4a/b* in these transgenic lines with modified GA signaling by RT-qPCR. As expected, the suppression of GA signaling in *WOX4a*$_{pro}$:Δ*RGL1* cambium significantly compromised the expression levels of *WOX4a/b*, with reductions of 68% and 59%, respectively (Figure 5A). The transcript abundance of the *WOX4* paralogs increased in response to the constitutive expression of *ARF7.2* but decreased in response to the knockout of *ARF7.2* and *ARF7.3* (Figure 5B). Overall, these results suggest that ARF7 functions as bridge to integrate GA and auxin signaling to regulate *WOX4* expression.

ARF7 directly binds to *WOX4* gene promoters and stimulates their expression

ARF proteins bind to auxin response elements (*AuxREs*) in the promoters of their downstream target genes to modulate their expression (Ulmasov et al., 1995). We, therefore, examined whether ARF7.2 directly binds to the *WOX4* promoters to regulate cambial activity. Sequence analysis revealed the presence of a series of canonical or core *AuxREs* in the *WOX4a/b* gene promoters (Figure 5C; Supplemental Figure S21A). Chromatin immunoprecipitation (ChIP)-qPCR assays showed that ARF7.2 associated with the promoters of these *WOX4* genes in vivo (Figure 5D; Supplemental Figure S21B). The affinity of ARF7.2 for canonical *AuxREs* was further verified by yeast one-hybrid (Y1H) assays. The mutation of the canonical *AuxRE* sequences in the promoters of *WOX4a* (Region I) and *WOX4b* (Region II) prevented the binding of ARF7.2 (Figure 5E; Supplemental Figure S21C). Additionally, the ARF7.2-binding capacity was demonstrated by a shift of labeled probes harboring Region I of the *WOX4a* promoter or Region II of the *WOX4b* promoter in an electrophoretic mobility shift assay (EMSA; Figure 5F, Supplemental Figure S21D). These results indicate that ARF7.2 binds to multiple AuxRE sites in the promoters of *WOX4a* and *WOX4b*.

We then examined ARF7-dependent regulation of *WOX4a/b* by transiently expressing effector–reporter constructs in *N. benthamiana* leaves. The co-transfection of *ARF7.2* activated the expression of the luciferase reporter gene driven by the canonical *AuxRE*-harboring Region I or II of the *WOX4a/b* promoters, respectively (Figure 5, G and H;

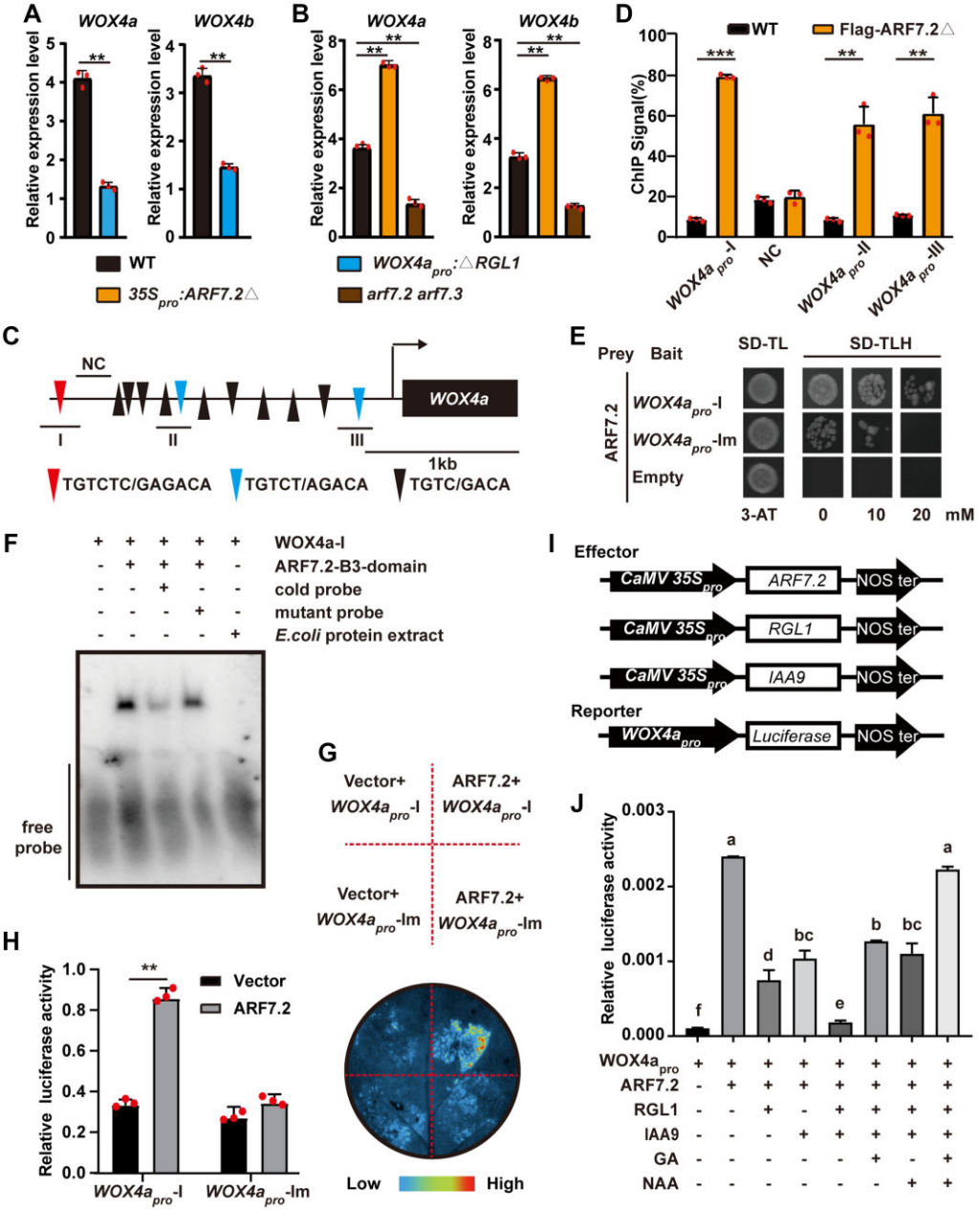

Figure 5 ARF7.2 directly regulates the expression of *WOX4a*. A and B, Relative expression levels of *WOX4a/b* in WT, *WOX4a*$_{pro}$:Δ*RGL1*, *35S*$_{pro}$:*ARF7.2*Δ, and *Cas9-ARF7.2/7.3* lines, as determined by RT-qPCR. Data are shown as means ± SD, $n = 3$. Asterisks indicate significant differences from WT seedlings, as determined by one-way ANOVA Dunnett's test: $^{**}P < 0.01$. C, Distribution of canonical and core *AuxREs* in the promoter region of *WOX4a*. Lines labeled I–III indicate *AuxRE*-containing fragments amplified by ChIP-qPCR, while NC represents the *AuxRE*-free negative control. D, ChIP-qPCR analysis of the binding of ARF7.2Δ protein fused with the FLAG tag to the promoter region of *WOX4a*. Leaf tissues of 2-month-old poplar plants were used. Error bars represent SD. One-way ANOVA Dunnett's test was performed to evaluate the differences between WT and Flag-ARF7.2Δ for each region. $^{**}P < 0.01$, $^{***}P < 0.001$. $n = 3$. E, ARF7 binds to the promoter region of *WOX4a*, as revealed by Y1H assays. SD-TL, synthetic medium lacking tryptophan and leucine; SD-TLH, synthetic medium lacking tryptophan, leucine, and histidine, supplemented with 0, 10, or 20 mM 3-AT, as indicated. F, ARF7 binds to the *AuxRE* element in the promoter of *WOX4a*, as revealed by EMSA. The B3-DNA-binding domain of ARF7.2 was used in this experiment. A 20× excess of unlabeled probe was used as a specific competitor (cold probe), whereas a 20× excess of unlabeled probe in which *AuxRE* was mutated to GTGTAG was used as an unspecific competitor (mutated probe). Protein extract of *E. coli* not expressing ARF7.2 was used as a negative control. G, Luciferase activity assay showing that ARF7.2 binds to the promoter region of *WOX4a*. The color-coded bar indicates the intensity of luciferase activity. H, Quantitative analysis of relative luciferase activity of the experimental materials in (G). Three randomly selected fields from three individual *N. benthamiana* plants per group were used for counting. The bars are means ± SD. Asterisks indicate significant difference using one-way ANOVA Dunnett's test. $^{**}P < 0.01$. In (E) and (G), the promoter fragment *WOX4a*$_{pro}$-I indicated in (C) was used. *WOX4a*$_{pro}$-Im harboring the mutated *AuxRE* (TGTCTG) was used as a negative control. I, Schematic diagrams of the effector, reporter, and reference constructs used in the luciferase activity assays. J, RGL1 and IAA9 combinatorially inhibit the targeted binding of ARF7.2 to the promoter of *WOX4a*. Each pair of effector and reporter plasmids was co-transformed into *N. benthamiana* leaf cells. Exogenous GA_4 (5 mg/mL) and/or NAA (10 mg/mL) was rubbed onto *N. benthamiana* leaves and the fluorescence measured after 8 h. Different letters above the bars represent significant differences among emasculated lines using one-way ANOVA Dunnett's test, $P < 0.01$.

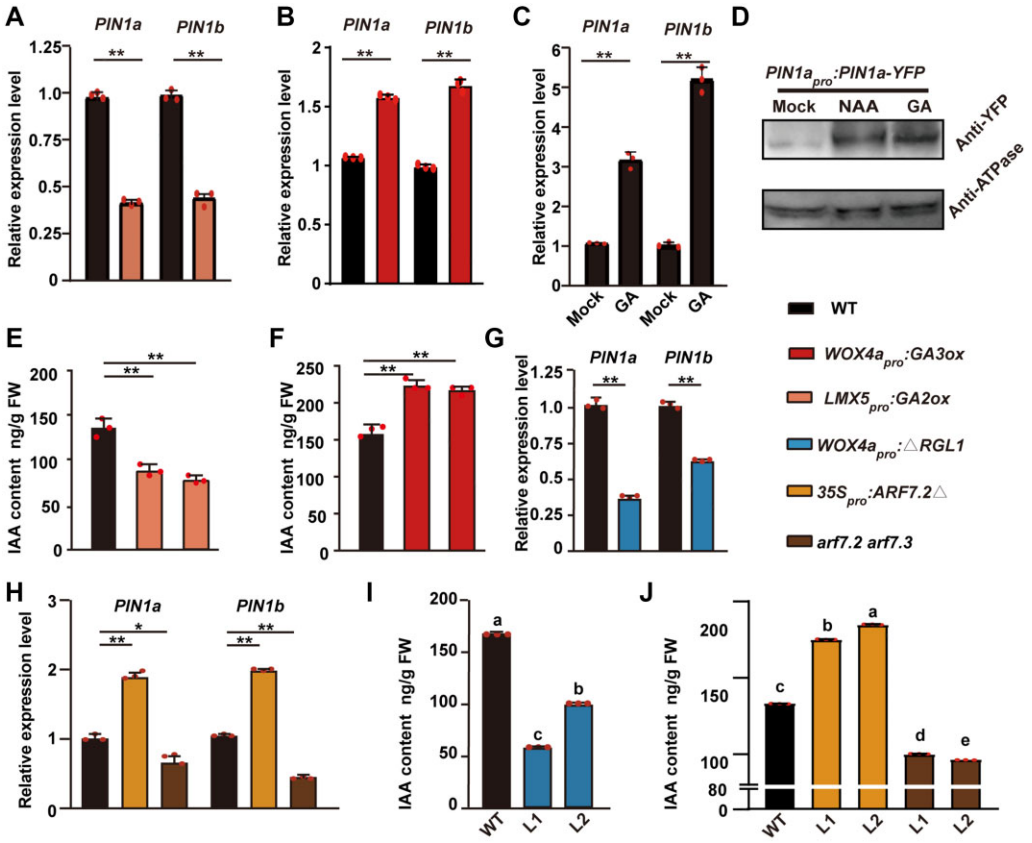

Figure 6 GA promotes auxin accumulation in the cambium by regulating *PIN1* expression. A and B, Relative expression levels of *PIN1a/b* in WT, *LMX5*$_{pro}$*:GA2ox*, and *WOX4a*$_{pro}$*:GA3ox* lines, WT plants under mock, GA, and IAA treatment (C), and WT, *WOX4a*$_{pro}$*:ΔRGL1*, *35S*$_{pro}$*:ARF7.2Δ*, and *Cas9-ARF7.2/7.3* lines (G and H), as determined by RT-qPCR. For (A, B, C, G, and H), data are shown as means ± SD, $n = 3$. Asterisks indicate statistically significant differences from WT seedlings, as determined by one-way ANOVA Dunnett's test: $^{**}P < 0.01$. D, Expression of *PIN1a* in plants after 3 days of mock, NAA, and GA treatment. YFP antibody was used to characterize the level of PIN1a protein, and H^+-ATPase was used as an internal control. E, F, I, and J, Quantification of IAA contents in WT, *LMX5*$_{pro}$*:GA2ox* and *WOX4a*$_{pro}$*:GA3ox* lines (E and F) and WT, *WOX4a*$_{pro}$*:ΔRGL1*, *35S*$_{pro}$*:ARF7.2Δ*, and *Cas9-ARF7.2/7.3* lines (I and J) by LC–MS/MS. Error bars represent ±SD. One-way ANOVA Dunnett's test was performed to evaluate significant differences between values in the WT and transgenic lines. $^{**}P < 0.01$. $n = 3$ (E and F). Different letters above the bars represent significant differences among emasculated lines, $P < 0.01$. $n = 3$ (I and J).

Supplemental Figure S21, E and F). In contrast, site-directed mutagenesis to disrupt the *AuxREs* in these promoter fragments abolished the transcriptional activation driven by ARF7.2 (Figure 5, G and H; Supplemental Figure S21, E and F). These results indicate that ARF7 directly regulates the expression of *WOX4* paralogs by binding to the *AuxREs* in their promoters.

To investigate the effects of the DELLA–ARF7–Aux/IAA ternary complex on the cooperative regulation of *WOX4* expression by GA and auxin, we performed a luciferase assay by transiently transfecting *N. benthamiana* leaves with a series of effector combinations (Figure 5I). The expression of the ARF7.2-activiated luciferase gene driven by the *WOX4a* promoter was significantly inhibited by co-transfection of either RGL1 or IAA9 (Figure 5J). Notably, when RGL1 and IAA9 were introduced into the leaves simultaneously, the ARF7.2-induced activation of *WOX4a* transcription was more severely inhibited compared to the introduction of RGL1 or IAA9 alone (Figure 5J). Furthermore, either GA or IAA treatment restored the expression of *WOX4a*, which was inhibited by RGL1 and IAA9 (Figure 5J). Similar results were obtained for the *WOX4b* promoter (Supplemental Figure S21G). Taken together, these results suggest that GA and auxin signaling combinatorially regulate *WOX4* expression in poplar, likely via the interactions of ARF7 with RGL1 and IAA9.

ARF7 regulates the expression of *PIN1* in poplar

A comprehensive survey of poplar *PIN* genes revealed the preferential expression of *PIN1* in the cambial zone (Liu et al., 2014) and the induction of its transcription in stems by exogenous auxin and GA treatment (Schrader et al., 2003; Bjorklund et al., 2007). We investigated the expression levels of *PIN1a* and *PIN1b* in these transgenic lines with altered GA content via RT-qPCR. These genes were downregulated in the *LMX5*$_{pro}$*:GA2ox* lines but upregulated in the *WOX4a*$_{pro}$*:GA3ox* lines (Figure 6, A and B), suggesting that endogenous GA positively regulates *PIN1* expression. In accordance with a previous report (Bjorklund et al., 2007), the transcript levels of the *PIN1* paralogs significantly increased

in response to GA treatment (Figure 6C). To examine PIN1 accumulation in stems, we introduced a construct expressing *YFP*-tagged *PIN1a* driven by its native promoter into poplar. Immunoblot assays showed that YFP-fused PIN1a accumulation was markedly induced by exogenous auxin and GA treatment compared to the negative control (Figure 6D).

We measured auxin levels in these transgenic lines with modulated GA content. Endogenous IAA levels decreased in *LMX5pro:GA2ox* stems but increased in *WOX4apro:GA3ox* stems compared to WT (Figure 6, E and F). We then treated WT plants with naphthylphthalamic acid (NPA), a chemical inhibitor of polar auxin transport, which inhibited cambial activity (Supplemental Figure S22, A–D). To determine whether auxin transport affects GA-stimulated cambial activity, we treated *WOX4a*$_{pro}$*:GA3ox* transgenic plants with NPA. Cambial development was strongly impaired by NPA treatment (Supplemental Figure S23A), which is similar to the effect of introducing IAA9m into the *WOX4a*$_{pro}$*:GA3ox* lines (Supplemental Figure S23, B–D). The expression of the *WOX4* paralogs was also significantly suppressed by NPA treatment (Supplemental Figure S23E). These results reveal the critical role of PIN-mediated polar auxin transport in GA-driven cambial activity.

Since the DELLA–ARF7–IAA9 module plays in a key role in orchestrating the transcriptional response to the crosstalk between GA and auxin signaling, we speculated that this module regulates the expression of *PIN1* paralogs. To test this idea, we monitored the expression of *PIN1a/b* in the *WOX4a*$_{pro}$*:RGL1*, *35S*$_{pro}$*:ARF7.2Δ* and *arf7.2 arf7.3* lines by RT-qPCR. Compared to WT, the expression of the *PIN1* paralogs was suppressed in the *WOX4a*$_{pro}$*:RGL1* lines (Figure 6G), suggesting that DELLAs negatively regulate *PIN1* expression. On the contrary, *PIN1* expression significantly increased in *35S*$_{pro}$*:ARF7.2Δ* transgenic plants but decreased in the *arf7.2 arf7.3* lines compared to WT (Figure 6H). Consistently, DELLA repressed the accumulation of endogenous IAA in stems, whereas ARF7 promoted its accumulation (Figure 6, I–J). These data suggest that the DELLA–ARF7–IAA9 module antagonistically regulates the expression of *PIN1*.

ARF7 directly regulates *PIN1a/b* expression by binding to their promoters

Since we demonstrated that ARF7 in the DELLA–AFR7–IAA9 complex functions as a direct mediator of auxin and GA signaling to coordinately regulate cambial activity, we asked if ARF7 is also capable of binding to the *PIN1* promoter and activating its expression. A number of canonical or core *AuxREs* are predicted to be present in the promoter sequences of both *PIN1* paralogs (Figure 7, A and B). Significant enrichment of *AuxRE*-containing promoter fragments of *PIN1a* or *PIN1b* was detected in *Flag-ARF7.2Δ* transgenic plants by ChIP-qPCR (Figure 7, C and D), suggesting that ARF7.2 binds to the *PIN1a/b* promoters in vivo. Furthermore, we detected the binding activity of ARF7.2 to the *AuxRE*-containing *PIN1a/b* promoter regions in Y1H assays, but this effect strongly decreased when the *AuxREs* were destroyed by site-directed mutagenesis (Figure 7E). To confirm this binding, we also performed EMSAs using purified recombinant proteins containing the B3 domain of ARF7.2 fused with GST-tag. Indeed, ARF7.2 bound to biotin-labeled probes of the *PIN1a/1b* promoters (Figure 7, F and G). Finally, to explore the effect of ARF7.2 on *PIN1a/1b* transcription, we performed a transient expression assay in *N. benthamiana* leaves. Luminescence imaging and quantification revealed that *PIN1a/1b*$_{pro}$*:LUC* reporter activity significantly increased in leaves transfected with the *35S*$_{pro}$*:ARF7.2* construct compared to the control vector (*pCXSN*, Chen et al., 2009) (Figure 7, H–K). When the *AuxREs* in the *PIN1a/1b* promoter fragments were mutated, this ARF7.2-driven activation was completely interrupted (Figure 7, H–K). Collectively, these results strongly support the notion that ARF7 directly regulates the expression of *PIN1a/1b* by binding to the *AuxRE* motifs in their promoters.

Discussion

ARF7 acts as a molecular bridge linking GA and auxin signaling to regulate cambial activity in poplar

The maintenance and differentiation of cambial activity are precisely regulated by a complex network of plant hormone signals and transcription factors (Fischer et al., 2019). Exogenous GA and auxin were previously shown to have a synergistic effect on cambial growth and induce common changes to the transcriptome in poplar (Digby and Wareing, 1966; Bjorklund et al., 2007). However, little is known about the molecular mechanism conferring the inter-connected activities of these two phytohormones in trees. In this study, we provided evidence for the interdependence of local GA and auxin signaling in the cambium and identified ARF7 as a molecular bridge of GA and auxin signaling pathways to regulate cambial development in poplar.

DELLA proteins are repressors of GA signaling that interact with various transcription factors to participate in diverse developmental processes (Sun, 2010; Gao et al., 2017). RGA, an Arabidopsis DELLA protein, is capable of binding to ARF6, ARF7, and ARF8, but not to ARF1 (Oh et al., 2014). By interacting with RGA, ARF6 is sequestered from the promoters of its target genes involved in hypocotyl elongation (Oh et al., 2014). In tomato (*Solanum lycopersicum*), DELLA interacts with ARF5, ARF7, ARF8, and ARF19, and its interactions with ARF7 mediate the crosstalk between GA and auxin signaling during fruit initiation (Hu et al., 2018). Here, our Y2H assays revealed physical interactions of poplar DELLAs with ARF6, ARF7, and ARF8 (Supplemental Figure S13B). Hence, the DELLA–ARF interactions might represent ubiquitous mechanisms directing the crosstalk between the GA and auxin pathways in vascular plants.

The MR domains of ARFs determine the transcriptional activity of these proteins (Guilfoyle and Hagen, 2007). Indeed, in this study, domain exchange revealed that the MR domain of ARF7 independently mediates the interaction

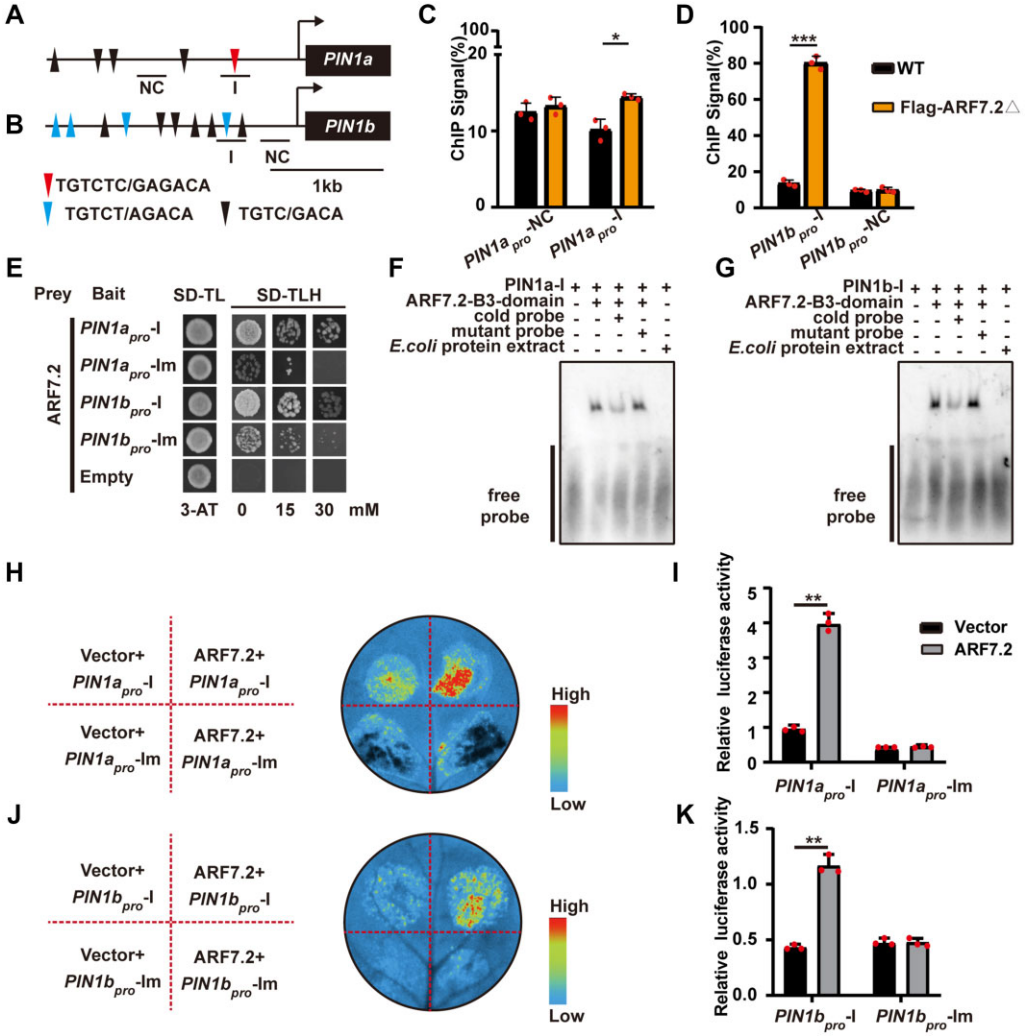

Figure 7 ARF7 directly regulates the expression of *PIN1* paralogs. A and B, Distribution of canonical and core AuxREs in the promoter regions of *PIN1a/b*. Black lines labeled I indicate AuxRE-containing fragments amplified by ChIP-qPCR, while NC represents the AuxRE-free negative control. C and D, ChIP-qPCR analysis of the binding of ARF7.2Δ protein fused with FLAG tag with the promoter regions of *PIN1a/b*. Leaf tissues of 2-month-old poplar plants were used. Error bars represent SD. One-way ANOVA Dunnett's test was performed to evaluate the differences between the values of WT and those of Flag-ARF7.2Δ for each region. $^{*}P < 0.05$, $^{***}P < 0.001$. $n = 3$. E, ARF7 binds to the promoter regions of *PIN1a/b*, as revealed by Y1H assays. SD-TL, synthetic medium lacking tryptophan and leucine; SD-TLH, synthetic medium lacking tryptophan, leucine, and histidine. Samples were supplemented with 0, 15, or 30-mM 3-AT, as indicated. F and G, ARF7 binds to AuxRE elements in the promoter regions of *PIN1a/b*, as determined by EMSA. The B3-DNA-binding domain of ARF7.2 was used for this experiment. A 20× excess of unlabeled probe was used as specific competitor (cold probe), whereas a 20× excess of unlabeled probe in which AuxRE was mutated to GTGTAG was used as an unspecific competitor (mutant probe). Protein extract of *E. coli* not expressing ARF7.2 was used as a negative control. H and J, Luciferase activity assay showing that ARF7.2 binds to the promoter regions of *PIN1a/b*. The color-coded bar indicates the intensity of luciferase activity. I and K Quantitative analysis of relative luciferase activity of the experimental materials in (H and J). Three randomly selected fields from three individual *N. benthamiana* plants per group were used to count means ± SD. Asterisks indicate significant difference using one-way ANOVA Dunnett's test. $^{**}P < 0.01$. In (E), (H), and (J), the promoter fragments are *PIN1a*$_{pro}$-I and *PIN1*b$_{pro}$-I indicated in (A) and (B) were used. *PIN1a*$_{pro}$-Im and *PIN1b*$_{pro}$-Im harboring the mutated AuxRE (TGTCTG) was used as a negative control.

of these proteins with DELLAs (Figure 3D). Thus, the specific affinity of this domain for DELLAs likely accounts for the DELLA-induced repression of ARF7-targeted genes. Similar to the well-established model of auxin signaling in Arabidopsis (Vanneste and Friml, 2009), the C-terminal PB1 domain of ARF7 was found to mediate its interactions with IAA9, an Aux/IAA protein (Supplemental Figure S14B). Therefore, various conserved domains of ARF7 are responsible for its physical interactions with DELLA and Aux/IAA repressors, conferring the structural basis for integrating GA and auxin signaling pathways in poplar. We provided multiple lines of evidence that poplar ARF7 interacts with RGL1 and IAA9 in a parallel manner through its distinct domains (Figure 3, E–I), thus forming a ternary complex. Similarly, during fruit expansion in tomato, ARF7 simultaneously interacts with DELLA and Aux/IAA proteins (Hu et al., 2018). Furthermore,

the knockout of poplar *ARF7* paralogs abolished the responsiveness of the cambium to exogenous GA or auxin, and a chimeric form of ARF7 that failed to interact with DELLAs restored the cambial activity that was inhibited by RGL1 (Figure 4). Taken together, our biochemical and genetic data support the role of ARF7 as a key link integrating GA and auxin signaling to regulate cambial activity in poplar.

ARF7 directly activates *WOX4* expression to mediate the synergistic effects of GA and auxin signaling on cambial activity

ARFs function as transcriptional switches of auxin-responsive genes, thereby playing diverse roles in orchestrating secondary growth. For instance, ARF6 and ARF8, which physically interact with DELLAs, play key roles in promoting xylem-dominated secondary growth in Arabidopsis hypocotyls (Fischer et al., 2019). In this study, even though ARF6 and ARF8 exhibited DELLA-binding activity (Supplemental Figure S12B), the *ARF6* and *ARF8* genes exhibited decreasing expression toward the internodes of poplar stems, allowing active radial thickening to be maintained (Supplemental Figure S12C), pointing to their involvement in certain developmental events prior to secondary growth. In Arabidopsis, ARF5 and ARF7 share overlapping and nonredundant functions to jointly regulate a series of auxin-dependent developmental programs (Hardtke et al., 2004). ARF5 is a versatile regulator of auxin-triggered vascular patterning in embryos and postembryonic organs (Hardtke and Berleth, 1998; Donner et al., 2009). In contrast to the prominent cambium defects caused by *ARF5* knockdown, the *arf7 arf19* double mutant showed no abnormality in secondary growth (Smetana et al., 2019). Our data show that the poplar *arf7.2 arf7.3* double mutant exhibits substantially reduced cambial activity and reduced sensitivity to GA and auxin signaling in terms of cambial cell division (Figure 4, A–D). These results demonstrate that ARF7 reinforces the maintenance of cambial activity in poplar stems.

WOX4, a crucial regulator of cambial cell proliferation, is targeted by CLE-PXY peptide signaling, representing parallel mechanisms of stem cell maintenance between the apical and lateral meristems (Hirakawa et al., 2010; Ji et al., 2010). The positive role of WOX4 in controlling CLE-PXY pathway-mediated cambial activity is conserved in poplar (Kucukoglu et al., 2017). In Arabidopsis, WOX4 promotes the differentiation and/or maintenance of cambial cells (Suer et al., 2011). ARF5 directly suppresses *WOX4* expression, thus recruiting cambial cells for secondary xylem production in Arabidopsis stems (Brackmann et al., 2018). We previously reported that ARF5 promotes secondary xylem formation from cambial stem cells in poplar by directly activating the expression of *HB7* and *HB8*, encoding homologous HD-ZIP III transcription factors (Xu et al., 2019). Here, we revealed that ARF7 rather than ARF5 interacts with DELLAs to help maintain cambial activity in poplar (Figure 3; Supplemental Figure S13B). ARF7 in the RGL1–ARF7–IAA9 ternary complex directly activates *WOX4a/b* expression in poplar by binding to the promoters of these genes, thus integrating GA- or auxin-stimulated *WOX4a/b* expression (Figure 5; Supplemental Figures S20 and S21). Therefore, the distinct protein partners and downstream target genes between ARF5 and ARF7 may account for their functional diversity during cambial maintenance in poplar. Collectively, the ARF7–WOX4 module provides a molecular connection that regulates cambial activity through the convergence of the GA, auxin, and CLE peptide signaling pathways.

GA stimulates PIN1-mediated polar auxin transport by activating ARF7

The exogenous application of both GA and auxin stimulated cambial growth in poplar more strongly than the application of these phytohormones alone and activated the expression of *PIN1* (Bjorklund et al., 2007). These findings point to a feedback mechanism underlying the crosstalk between GA and auxin signaling in the cambium. However, the key components that mediate this feedback remain unclear. Here, we showed that ARF7 regulates the expression of *PIN1a/1b* by directly binding to their promoters and interacts with the DELLA protein RGL1 (Figures 6 and 7). These findings identify DELLA-ARF7 as the mediator of the GA-dependent regulation of PIN1-mediated polar auxin transport.

Auxin canalization is thought to underlie the positive feedback between auxin signaling and polar auxin transport (Sauer et al., 2006; Ravichandran et al., 2020). In accordance with this hypothesis, the production of transcripts of poplar *PIN1* homologs, which are enriched in the cambium, was significantly induced by exogenous auxin treatment. ARF7, a transcriptional integrator of local GA and auxin signaling in the cambium, directly activates the expression of *PIN1* paralogs in poplar (Figure 7), providing a molecular pathway for the GA-dependent regulation of auxin canalization via modifying the feedback regulation of polar auxin transport. In contrast to the local auxin peak in the cambium, the concentration of GA is highest in developing xylem and gradually decreases in the cambium (Immanen et al., 2016). GA-stimulated cambial activity and *WOX4* expression were largely compromised by treatment with a polar auxin transport inhibitor (Supplemental Figure S16), suggesting that polar auxin transport plays an essential role in GA-triggered cambial development. The GA-promoted turnover of DELLA allows ARF7 to exert positive feedback on *PIN1* expression and auxin enrichment in the cambium, which in turn further activate the expression of its target genes. Therefore, RGL1, ARF7, and PIN1 constitute an amplification cascade of GA signaling that regulates cambial activity via protein interactions and a feedback loop.

In conclusion, we propose a working model that provides mechanistic insights into the role of the crosstalk between GA and auxin signaling in cambial activity in poplar stems (Figure 8). During the maintenance of cambial activity in poplar stems undergoing secondary growth, ARF7 acts as a core component that integrates GA and auxin signaling

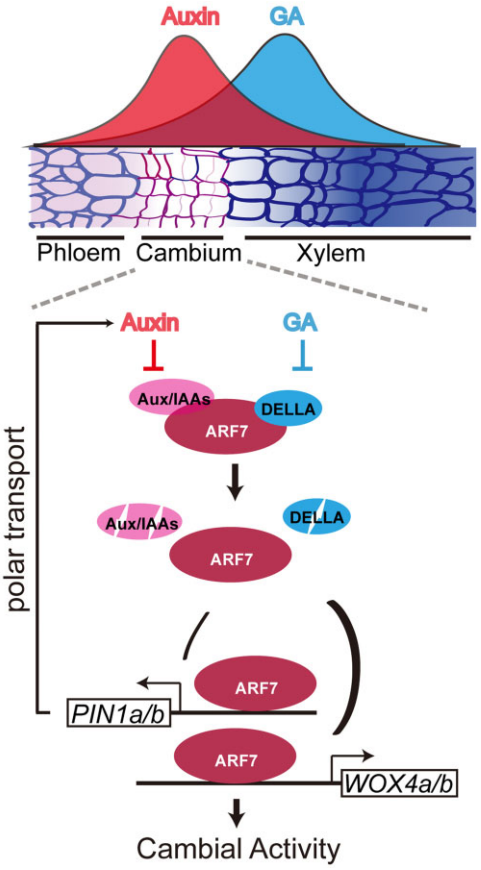

Figure 8 Model of the crosstalk between the GA and auxin signaling pathways in regulating cambial activity during wood development. High levels of auxin and GA accumulate in the cambium and developing xylem, respectively, and both are present in the cambium. Auxin degrades Auxin/IAA proteins, and GA destabilizes DELLA proteins, which compromise the DELLA–ARF7–Auxin/IAA ternary complex and relieve the inhibition of ARF7 activity. ARF7 directly regulates *WOX4a/b* expression to promote cambial activity. ARF7 also directly regulates *PIN1a/b* expression to promote high auxin accumulation in the cambial zone.

through physical interactions with DELLA and Aux/IAA proteins. DELLA proteins bind to ARF7s and prevent them from activating downstream gene expression. Cambium-localized GA triggers local GA signaling to destabilize DELLA proteins, thereby releasing ARF7 to activate its direct targets, including *WOX4* and *PIN1*, encoding a key cambial regulator and polar auxin efflux transporter, respectively. This working model is supported by the finding that the ARF7 variant without the ability to bind to DELLAs restored the defects caused by the dominant-negative form of DELLAs (Figure 4). The feedback circuit of ARF7 and PIN1 stimulates auxin-triggered turnover of Aux/IAA proteins in the cambium, thereby further releasing the ability of ARF7 to activate *WOX4* expression. Our findings indicate that ARF7 physically interacts with DELLA and Aux/IAA proteins to form a ternary complex. Therefore, the DELLA–ARF7–Aux/IAA complex coordinates the crosstalk of GA and auxin signaling to regulate cambial activity in poplar by directly regulating the expression of *WOX4*.

Materials and methods

Plant materials and transformation

Genetic transformation of *P. tomentosa* was performed via *Agrobacterium*-mediated infiltration of leaf disks as described previously (Jia et al., 2010). Positive transgenic lines for each construct were identified by PCR genotyping using gene-specific primers (Supplemental Data Set 1). For phenotypic analysis, seedlings were transferred to soil in pots and cultivated in the greenhouse at 25°C under long-day conditions (16-h light/8-h dark, 10,000 lux supplemental light (20W T8-type LED)) and 60% humidity for 2 months.

Gene cloning and plasmid construction

The promoter sequences of *LMX5* (1,823-bp upstream of ATG) and *WOX4a* (1,904 bp upstream of ATG) were amplified from genomic DNA of *Populous tomentosa* using PrimerSTAR Max DNA Polymerase (R045A; TAKARA, Shiga, Japan) with specific primer pairs. The *CaMV35S* promoter in the *pCAMBIA1305* vector was removed by digestion with EcoRI and BamHI (#R3101S & #R3136M, New England Biolabs, Beijing, China) and replaced by the *LMX5* or *WOX4a* promoter using a DNA Ligation Kit (6022Q, TAKARA, Japan). The full-length coding sequences (CDSs) of *GA3ox*, *GA2ox*, *DELLAs*, *ARFs*, and *PIN1a* were amplified from *P. tomentosa* cDNA using specific primer pairs. The sequence 51 bp after the 126th position was deleted by overlap-PCR to generate a mutant form of *RGL1* designated *ΔRGL1*. The CDS of β-glucuronidase (GUS) downstream of the *LMX5* or *WOX4a* promoter was replaced by those of *GA3ox*, *GA2ox*, or *ΔRGL1*. The full-length CDSs of *ARF7.2* and *RGL1* were cloned into the *pCXSN-Flag* and *pCXDG* vectors (Chen et al., 2009). The *ARF7.2Δ* sequence, harboring the 1,983 N-terminal nucleotides of *ARF7.2*, was amplified from *pCXSN-Flag-ARF7.2* and inserted into the *pCXSN* vector (Chen et al., 2009). The 771- to 1,983-bp *ARF7.2* CDS and the 801- to 1,989-bp *ARF5.1* CDS were replaced by overlap-PCR to form $ARF7.2^{757}$ and $ARF5.1^{575}$, respectively, and inserted into *pCXSN*. The binary pYLCRISPR/Cas9 multiplex genome targeting vector system (Fan et al., 2015) was used to edit the poplar genome to generate mutants of *ARF7.2/7.3*. The CRISPR/Cas9 target sites of *ARF7.2* and *ARF7.3* were designed using the online tool ZiFiT Targeter version 4.2 (http://zifit.partners.org/ZiFiT/Introduction.aspx) (Sander et al., 2010). Four common sequences of *ARF7.2* and *ARF7.3* were selected and assembled into the Cas9/sgRNA construct as described previously (Fan et al., 2015). The *YFP* gene without the stop codon was cloned from the *pEarleyGate 101* vector and inserted after the 1,251-bp CDS of *PIN1a* so that YFP was fused to the hydrophilic loop of PIN1a. The *PIN1a* promoter (2,371-bp upstream of ATG) and *PIN1a-YFP* were inserted into the *pCAMBIA1305* vector to generate the

PIN1a$_{pro}$*:PIN1a-YFP* plasmid. The primer sequences are listed in Supplemental Data Set 2.

Phytohormone and chemical treatments

For phytohormone treatment, 2-month-old poplar trees were decapitated at the eighth internode, and axillary buds were removed to avoid interference from possible sources of plant hormones from lateral branches. Lanolin with IAA (Sigma-Aldrich, St Louis, MO, USA) and GA_4 (Sigma-Aldrich) was applied to the cut end as described previously (Bjorklund et al., 2007). In addition, 1-month-old plantlets were treated with 5-μM 1-N-NPA (N131601; Aladdin, China) under hydroponic conditions for 30 days before phenotypic analysis.

Phylogenetic analysis

The amino acid sequences of DELLA homologs from *A. thaliana* and *P. trichocarpa* were aligned with ClustalW to build a phylogenetic tree (Supplemental File S1). The phylogenetic tree was constructed based on the neighbor-joining method in MEGA version 9. The parameters used were as follows: complete deletion and bootstrap (1,000 replicates). The phylogenetic tree of ARFs was constructed using the same method (Supplemental File S2).

Cross-sectioning and histological staining

The eighth internodes of different transgenic plants were sectioned using a vibrating blade microtome (VT1000s; Leica, Wetzlar, Germany) and stained with 0.05% (w/v) toluidine blue for 5 min. The cross-sections were photographed under a microscope (Zeiss), and anticlinal cell divisions were analyzed as described previously (Schrader et al., 2003; Nilsson et al., 2008). The calculated frequency of anticlinal divisions represents the percentage of anticlinal divisions to the total number of cells in the corresponding cambium cell file.

RNA extraction and RT-qPCR

Total RNA was extracted from the stems of 2-month-old poplar trees using a Biospin Plant Total RNA Extraction Kit (Bioflux, China). Complementary DNA was synthesized using a PrimeScript RT reagent kit with gDNA Eraser (0047A, TAKARA, Dalian, China) according to the manufacturer's instructions. RT-qPCR was performed using Hieff qPCR SYBR Green Master Mix (11201ES08, YEASEN, China) according to the manufacturer's instructions in a qTOWER3G IVD Real-Time PCR machine (Analytik Jena AG, Germany). The poplar *UBIQUITIN* gene was used as the reference gene. The primer sequences are listed in Supplemental Data Set 2.

Protein extraction and immunoblot analysis

Membrane proteins were extracted from the samples using a Minute Plasma Membrane Protein Isolation Kit (SM-005-p, Invent, USA). PIN1a-YFP protein was detected by immunoblot analysis using monoclonal anti-GFP antibody (ab290, Abcam, China). As a loading control, the antibody against H^+-ATPase (AS07 260, Agrisera, Sweden) was used as the internal standard to detect membrane proteins.

Measurement of GA and IAA contents

GA and IAA were extracted from ~0.5-g poplar stem samples. After harvest, the tissues were immediately immersed in liquid nitrogen and the fresh weight recorded. GA and IAA were extracted from the samples as described previously (Yoshimoto et al., 2009). About 10 ng [$^2H_2$] GA_4 and/or 50 ng of [$^{13}C_6$] IAA were added to the samples as internal standards. The homogenates were transferred into 15-mL tubes and extracted overnight at 4°C. The solutions were evaporated to dryness under a vacuum using a concentrator (Savant ISS110 SpeedVac; ThermoFisher Scientific, Waltham, MA, USA) at 40°C. The samples were redissolved in 100 μL of 10% methanol and filtered for quantification using an LC–ESI–MS/MS system (4000 Q-Trap; Sciex, Framingham, MA, USA) as described previously (Zeng et al., 2019).

LCI assay

LCI assays were carried out via transient transfection of *N. benthamiana* leaves as previously described (Chen et al., 2008). The full-length CDSs of *IAA9m*, *RGL1*, *ARF7.2*, *ARF7.2Δ*, and *ARF7.2*^{757} were fused with the C- and/or N-terminal fragment of luciferase (cLUC or nLUC); the primer sequences are listed in Supplemental Data Set 2. Agrobacteria containing individual constructs were mixed and infiltrated into *N. benthamiana* leaves. The infiltrated leaves were incubated in the dark for 12 h, followed by 48 h in the light, sprayed with 1-mM D-luciferin potassium salt solution (40902ES01, YEASEN, China), and observed using a Fusion SL4 spectral imaging system (Vilber, Beijing, China).

Y1H, Y2H, and Y3H assays

To examine the binding of ARF7.2 to the target gene promoters, the CDS of *ARF7.2* was amplified and ligated into the yeast expression vector *pGADT7*. The *WOX4a/b* and *PIN1a/b* promoter fragments were ligated into *pHIS2*. The constructs were co-transformed into yeast strain Gold1 using the Clontech Yeast Hybrid System (Clontech, Palo Alto, CA, USA). The transformants were grown on SD medium lacking tryptophan and leucine (SD-TL) and selected on SD medium lacking tryptophan, leucine, and histidine (SD-TLH) with 3-amino-1,2,4-triazole (3-AT).

Y2H and Y3H assays were performed according to the manufacturer's instructions (Clontech, Palo Alto, CA, USA). The CDSs of *DELLAs* and *ARFs* were individually ligated into BamHI/EcoRI double-digested *pGADT7* or *pGBKT7* via homologous recombination using a ClonExpress II One Step Cloning Kit (C112-01, Vazyme, China). The constructs were co-transformed into yeast strain Gold2. Following growth on SD-TL medium, transformants were selected on SD medium lacking tryptophan, histidine, leucine, and adenine (SD-THLA). For the Y3H assays, the *IAA9* CDS was fused to the GAL4-binding domain, and the full-length CDS of *ARF7.2* was inserted downstream of the *MET25* promoter in *pBridge*. The constructs were co-transformed into yeast

strain Gold2 and screened on SD-THLA. The presence or absence of methionine was used to regulate the activity of the *MET25* promoter. The primer sequences are listed in Supplemental Data Set 2.

BiFC assay

For the BiFC assays, the full-length CDSs of *RGA1*, *RGL1*, and *ARF7.2* were ligated into *pXY104* or *pXY106* in-frame with cYFP or nYFP using a ClonExpress II One Step Cloning Kit (C112-01, Vazyme, China). Agrobacteria containing individual constructs were co-transformed into *N. benthamiana* leaves, and YFP fluorescent signals were observed under a laser confocal microscope (589 FV1200, Olympus, Japan). The primer sequences are listed in Supplemental Data Set 2.

Co-IP assays

For the Co-IP assays, RGL1 was fused with the GFP tag in the *pCXDG* vector, IAA9m was fused with the HA tag in the *pCXSN-HA* vector, and ARF7.2 was fused with the Flag tag in the *pCXSN-Flag* vector (Chen et al., 2009). *Agrobacterium* strain GV3101 cells containing individual constructs were co-infiltrated into *N. benthamiana* leaves. Total proteins were extracted from the samples as described previously (Wang et al., 2017). Protein A agarose gel (10279981, GE Healthcare, Sweden) was used for preclearing. Following immunoprecipitation with 3 μg GFP-specific antibody (ab290, Abcam, China), the beads were washed 6–8 times with lysis buffer and collected for immunoblot detection. The fusion protein was detected by immunoblotting using monoclonal anti-Flag antibody (F1804, Sigma, China) and monoclonal anti-HA antibody (H9658, Sigma, China). The primer sequences are listed in Supplemental Data Set 2.

Promoter activation assay

The promoter sequences of *WOX4a* (1,904-bp upstream of ATG) and *WOX4b* (1,900-bp upstream of ATG) were amplified from *P. tomentosa* genomic DNA with gene-specific primers (Supplemental Data Set 2) using PrimerSTAR Max DNA Polymerase (R045A, TAKARA, Japan) and fused with the luciferase reporter in the *pGreen0800* vector (Hellens et al., 2005). The full-length CDSs of *ARF7.2*, *RGL1*, and *IAA9* were amplified and separately cloned into *pCXSN* as effector plasmids. *N. benthamiana* leaves were transformed with Agrobacteria containing the effectors and reporters as described above. After 3 days of infiltration, promoter activation was measured using a Dual Luciferase Assay kit (E1910; Promega, USA) according to the manufacturer's instructions.

ChIP-qPCR

For ChIP assays, leaves from 2-month-old WT and ARF7.2Δ−FLAG overexpressing poplar plants were harvested, cross-linked with 1% formaldehyde under a vacuum, and ground in liquid nitrogen. The chromatin was sheared into ∼500-bp fragments by ultrasonication, and anti-Flag antibody (A8592; Sigma, China) was used for immunoprecipitation as previously described (Yang et al., 2012). qPCR was performed to identify the binding sites of ARF7.2 in the promoter regions of *WOX4/b* and *PIN1a/b*. All primers used in ChIP analysis are listed in Supplemental Data Set 2.

EMSA

The coding region of the B3-domain of ARF7.2 was fused in-frame with GST in the *pGEX-6p-2* vector and expressed in *Escherichia coli* Rosetta (DE3) cells. The recombinant B3-GST protein used for EMSA was purified using GST-Sep Glutathione Agarose Resin 4FF (20508ES10, YEASEN, China). The probes were labeled with biotin using an EMSA Probe Biotin Labeling Kit (GS008, Beyotime, China). Recombinant protein was incubated with labeled probes at room temperature for 20 min, and unlabeled probes were used as a competitor to examine the specificity of binding. Protein/promoter fragment complexes were separated by electrophoresis on a native 4% acrylamide gel. The DNA was electroblotted onto nitrocellulose membranes and detected using a Chemiluminescent EMSA Kit (GS009, Beyotime, China). EMSA images were photographed using a Fusion SL4 spectral imaging system (Vilber, Beijing, China).

RNA in situ hybridization

The partial sequences of *ARF7.2* (205 bp) and *RGL1* (271 bp) were amplified from *P. tomentosa* cDNA to prepare the probes for RNA in situ hybridization (Supplemental Data Set 2). The probes were labeled using a DIG RNA Labeling Kit (11175025910; Roche, USA) following the manufacturer's instructions. Stem sections from the sixth internodes of 3-month-old *P. tomentosa* plants were used for hybridization, followed by immunological detection as described previously (Sang et al., 2012).

Statistical analyses

Quantitative data for gene expression, plant hormone contents, fluorescence intensities, luciferase activity, and physiological measurements were examined for statistically significant differences using *t* test, one-way or two-way ANOVA as described in the corresponding figure legends. The results are shown in Supplemental Data Set 1. For ANOVA, Dunnett's test was performed to distinguish significant differences between pairwise samples ($^{*}P < 0.05$; $^{**}P < 0.01$; and $^{***}P <$ a0.001).

Accession numbers

The GenBank accession numbers of the *P. tomentosa* genes used in this study are as follows: *ARF5.1* (MH352401), *ARF7.2* (OK544549), *GA2ox* (OK544560), *GA3ox* (OK544559), *IAA9* (MH345700), *PIN1a* (OK544554), *PIN1b* (OK544555), *RGA1* (OK544550), *RGA2* (OK544551), *RGL1* (OK544552), *RGL2* (OK544553), *WOX4a* (OK544561), *WOX4b* (OK544562).

Supplemental data

The following materials are available in the online version of this article.

Supplemental Figure S1. Cambium phenotypes of stem tissues after the application of IAA and GAs to *P. tomentosa*.

Supplemental Figure S2. Generation of transgenic lines with various levels of GA during wood formation in *P. tomentosa*.

Supplemental Figure S3. Wood phenotypes in plants with various GA levels.

Supplemental Figure S4. Cambium phenotypes resulting from overexpression of $LMX5_{pro}$:*GA3ox* and $LMX5_{pro}$:*GA2ox* in *P. tomentosa*.

Supplemental Figure S5. Expression analysis of *DELLAs* during wood formation.

Supplemental Figure S6. Deleting the DELLA domain causes RGL1 to lose its function in the GA signaling pathway.

Supplemental Figure S7. Generation and phenotypic analysis of $WOX4a_{pro}$:*ΔRGL1* transgenic lines.

Supplemental Figure S8. Phenotypic analysis of the cambiums of $WOX4a_{pro}$:*ΔRGL1* transgenic lines.

Supplemental Figure S9. Statistics of the number of cambium layers and the frequency of anticlinal divisions in $LMX5_{pro}$:*GA2ox* transgenic lines under mock and IAA treatment.

Supplemental Figure S10. Generation and phenotypic analysis of $WOX4a_{pro}$:*GA3ox* and $WOX4a_{pro}$:*IAA9m*≫ $WOX4a_{pro}$:*GA3ox* transgenic lines.

Supplemental Figure S11. Statistics of the number of cambium layers and the frequency of anticlinal divisions in $WOX4a_{pro}$:*GA3ox* and $WOX4a_{pro}$:*IAA9m*≫ $WOX4a_{pro}$:*GA3ox* transgenic lines.

Supplemental Figure S12. Statistics of the number of cambium layers and the frequency of anticlinal divisions in WT and $WOX4a_{pro}$: *ΔRGL1* transgenic lines under mock, GA, and IAA treatment.

Supplemental Figure S13. Analysis of the expression of ARFs and their interactions with DELLAs.

Supplemental Figure S14. Analysis of the self-activation of ARF7.2/ARF5.1 and their interactions with IAA9.

Supplemental Figure S15. Identification of *ARF7.2*-overexpressing and knockdown transgenic lines.

Supplemental Figure S16. Phenotypic observation of *ARF7.2*-overexpressing and knockdown transgenic lines.

Supplemental Figure S17. Statistics of the number of cambium layers and the frequency of anticlinal divisions in *arf7.2 arf7.3* lines under mock, GA, and IAA treatment.

Supplemental Figure S18. Generation and phenotypic analysis of $35S_{pro}$:*RGL1* and $35S_{pro}$:$ARF7.2^{757}$≫$35S_{pro}$:*RGL1* transgenic lines.

Supplemental Figure S19. Statistics of the number of cambium layers and the frequency of anticlinal divisions in $35S_{pro}$:*RGL1* and $35S_{pro}$:$ARF7.2^{757}$≫$35S_{pro}$:*RGL1* transgenic lines.

Supplemental Figure S20. Screening of co-expressed genes induced by GA and auxin treatment involved in regulating cambial activity.

Supplemental Figure S21. ARF7.2 directly regulates the expression of *WOX4b*.

Supplemental Figure S22. Cambium phenotypes of WT under NPA treatment.

Supplemental Figure S23. Cambium phenotypes and *WOX4a/b* expression in $WOX4a_{pro}$:*GA3ox* transgenic lines under NPA treatment.

Supplemental Data Set 1. ANOVA and *t* test results.

Supplemental Data Set 2. Sequences of the oligonucleotide primers and probes used in this study.

Supplemental File S1. Alignment data used to generate the phylogenetic tree in Supplemental Figure S5A.

Supplemental File S2. Alignment data used to generate the phylogenetic tree in Supplemental Figure S13A.

Acknowledgments

We thank Dr. Ning Wei (Southwest University, China) for helpful comments and Dr. Mi Zhang and Yaohua Li (Southwest University, China) for help in measuring plant hormone contents.

Funding

This work was supported by grants from the National Key Research and Development Program (2021YFD2200204), National Science Foundation of China (31870657, 32071791, and 31870175), Chongqing Youth Top Talent Program (CQYC201905028), and Graduate Research and Innovation Projects of Chongqing (CYB19081).

Conflict of interest statement. None declared.

References

An F, Zhang X, Zhu Z, Ji Y, He W, Jiang Z, Li M, Guo H (2012) Coordinated regulation of apical hook development by gibberellins and ethylene in etiolated Arabidopsis seedlings. Cell Res **22**: 915–927

Ben-Targem M, Ripper D, Bayer M, Ragni L (2021) Auxin and gibberellin signaling cross-talk promotes hypocotyl xylem expansion and cambium homeostasis. J Exp Bot **72**: 3647–3660

Bjorklund S, Antti H, Uddestrand I, Moritz T, Sundberg B (2007) Cross-talk between gibberellin and auxin in development of *Populus* wood: gibberellin stimulates polar auxin transport and has a common transcriptome with auxin. Plant J **52**: 499–511

Brackmann K, Qi J, Gebert M, Jouannet V, Schlamp T, Grunwald K, Wallner ES, Novikova DD, Levitsky VG, Agusti J, Sanchez P, Lohmann JU, Greb T (2018) Spatial specificity of auxin responses coordinates wood formation. Nat Commun **9**: 875

Burroughs AM, Balaji S, Iyer LM, Aravind L (2007) Small but versatile: the extraordinary functional and structural diversity of the beta-grasp fold. Biol Direct **2**: 18

Campbell L, Turner S (2017) Regulation of vascular cell division. J Exp Bot **68**: 27–43

Chaffey N, Cholewa E, Regan S, Sundberg B (2002) Secondary xylem development in Arabidopsis: a model for wood formation. Physiol Plant **114**: 594–600

Chen H, Zou Y, Shang Y, Lin H, Wang Y, Cai R, Tang X, Zhou JM (2008) Firefly luciferase complementation imaging assay for protein-protein interactions in plants. Plant Physiol **146**: 368–376

Chen SB, Songkumarn P, Liu JL, Wang GL (2009) A versatile zero background T-vector system for gene cloning and functional genomics. Plant Physiol **150**: 1111–1121

Digby J, Wareing PF (1966) Effect of applied growth hormones on cambial division and differentiation of cambial derivatives. Ann Bot-Lond **30**: 539

Dill A, Jung HS, Sun TP (2001) The DELLA motif is essential for gibberellin-induced degradation of RGA. Proc Natl Acad Sci USA **98**: 14162–14167

Dinesh DC, Villalobos L, Abel S (2016) Structural biology of nuclear auxin action. Trends Plant Sci **21**: 302–316

Donner T, Sherr I, Scarpella E (2009) Regulation of preprocambial cell state acquisition by auxin signaling in Arabidopsis leaves. Development **136**: 3235–3246

Etchells JP, Provost CM, Mishra L, Turner SR (2013) WOX4 and WOX14 act downstream of the PXY receptor kinase to regulate plant vascular proliferation independently of any role in vascular organisation. Development **140**: 2224–2234

Fan D, Liu T, Li C, Jiao B, Li S, Hou Y, Luo K (2015) Efficient CRISPR/Cas9-mediated targeted mutagenesis in populus in the first generation. Sci Rep **5**: 12217

Fischer U, Kucukoglu M, Helariutta Y, Bhalerao RP (2019) The dynamics of cambial stem cell activity. Annu Rev Plant Biol **70**: 293–319

Gao X, Zhang Y, He Z, Fu X (2017) Gibberellins. *In* J Li, C Li, SM Smith, eds, Hormone Metabolism and Signaling in Plants. Elsevier Ltd, New York, NY, pp 107–160

Gouwentak CA (1941) Cambial activity as dependent on the presence of growth hormone and the non-resting condition of stems. P K Ned Akad Wetensc **44**: 654–663

Greb T, Lohmann JU (2016) Plant stem cells. Curr Biol **26**: R816–R821

Guilfoyle TJ, Hagen G (2007) Auxin response factors. Curr Opin Plant Biol **10**: 453–460

Han S, Cho H, Noh J, Qi JY, Jung HJ, Nam H, Lee S, Hwang D, Greb T, Hwang I (2018) BIL1-mediated MP phosphorylation integrates PXY and cytokinin signalling in secondary growth. Nat Plants **4**: 605–614

Hardtke CS, Berleth T (1998) The Arabidopsis gene MONOPTEROS encodes a transcription factor mediating embryo axis formation and vascular development. EMBO J **17**: 1405–1411

Hardtke CS, Ckurshumova W, Vidaurre DP, Singh SA, Stamatiou G, Tiwari SB, Hagen G, Guilfoyle TJ, Berleth T (2004) Overlapping and non-redundant functions of the Arabidopsis auxin response factors MONOPTEROS and NONPHOTOTROPIC HYPOCOTYL 4. Development **131**: 1089–1100

Hellens RP, Allan AC, Friel EN, Bolitho K, Grafton K, Templeton MD, Karunairetnam S, Gleave AP, Laing WA (2005) Transient expression vectors for functional genomics, quantification of promoter activity and RNA silencing in plants. Plant Methods **1**: 13

Hirakawa Y, Kondo Y, Fukuda H (2010) TDIF peptide signaling regulates vascular stem cell proliferation via the WOX4 homeobox gene in Arabidopsis. Plant Cell **22**: 2618–2629

Hu JH, Israeli A, Ori N, Sun TP (2018) The Interaction between DELLA and ARF/IAA mediates crosstalk between gibberellin and auxin signaling to control fruit initiation in tomato. Plant Cell **30**: 1710–1728

Immanen J, Nieminen K, Smolander OP, Kojima M, Alonso Serra J, Koskinen P, Zhang J, Elo A, Mahonen AP, Street N, et al. (2016) Cytokinin and auxin display distinct but interconnected distribution and signaling profiles to stimulate cambial activity. Curr Biol **26**: 1990–1997

Israelsson M, Sundberg B, Moritz T (2005) Tissue-specific localization of gibberellins and expression of gibberellin-biosynthetic and signaling genes in wood-forming tissues in aspen. Plant J **44**: 494–504

Jeon HW, Cho JS, Park EJ, Han KH, Choi YI, Ko JH (2016) Developing xylem-preferential expression of PdGA20ox1, a gibberellin 20-oxidase 1 from *Pinus densiflora*, improves woody biomass production in a hybrid poplar. Plant Biotechnol J **14**: 1161–1170

Ji J, Strable J, Shimizu R, Koenig D, Sinha N, Scanlon MJ (2010) WOX4 promotes procambial development. Plant Physiol **152**: 1346–1356

Jia Z, Sun Y, Yuan L, Tian Q, Luo K (2010) The chitinase gene (*Bbchit1*) from *Beauveria bassiana* enhances resistance to *Cytospora chrysosperma* in *Populus tomentosa* Carr. Biotechnol Lett **32**: 1325–1332

Kucukoglu M, Nilsson J, Zheng B, Chaabouni S, Nilsson O (2017) WUSCHEL-RELATED HOMEOBOX4 (WOX4)-like genes regulate cambial cell division activity and secondary growth in *Populus* trees. New Phytol **215**: 642–657

Little CHA, Savidge RA (1987) The role of plant-growth regulators in forest tree cambial growth. Plant Growth Regul **6**: 137–169

Little CHA, MacDonald JE, Olsson O (2002) Involvement of indole-3-acetic acid in fascicular and interfascicular cambial growth and interfascicular extraxylary fiber differentiation in *Arabidopsis thaliana* inflorescence stems. Int J Plant Sci **163**: 519–529

Liu B, Zhang J, Wang L, Li J, Zheng H, Chen J, Lu M (2014) A survey of Populus PIN-FORMED family genes reveals their diversified expression patterns. J Exp Bot **65**: 2437–2448

Love J, Bjorklund S, Vahala J, Hertzberg M, Kangasjarvi J, Sundberg B (2009) Ethylene is an endogenous stimulator of cell division in the cambial meristem of *Populus*. Proc Natl Acad Sci USA **106**: 5984–5989

Marin-de la Rosa N, Sotillo B, Miskolczi P, Gibbs DJ, Vicente J, Carbonero P, Onate-Sanchez L, Holdsworth MJ, Bhalerao R, Alabadi D, et al. (2014) Large-scale identification of gibberellin-related transcription factors defines group VII ETHYLENE RESPONSE FACTORS as functional DELLA partners. Plant Physiol **166**: 1022–1032

Matsumoto-Kitano M, Kusumoto T, Tarkowski P, Kinoshita-Tsujimura K, Vaclavikova K, Miyawaki K, Kakimoto T (2008) Cytokinins are central regulators of cambial activity. Proc Natl Acad Sci USA **105**: 20027–20031

Mauriat M, Moritz T (2009) Analyses of GA20ox- and GID1-over-expressing aspen suggest that gibberellins play two distinct roles in wood formation. Plant J **58**: 989–1003

Nilsson J, Karlberg A, Antti H, Lopez-Vernaza M, Mellerowicz E, Perrot-Rechenmann C, Sandberg G, Bhalerao RP (2008) Dissecting the molecular basis of the regulation of wood formation by auxin in hybrid aspen. Plant Cell **20**: 843–855

Oh E, Zhu JY, Bai MY, Arenhart RA, Sun Y, Wang ZY (2014) Cell elongation is regulated through a central circuit of interacting transcription factors in the Arabidopsis hypocotyl. Elife **3**: e03031

Peng JR, Carol P, Richards DE, King KE, Cowling RJ, Murphy GP, Harberd NP (1997) The Arabidopsis GAI gene defines a signaling pathway that negatively regulates gibberellin responses. Gene Dev **11**: 3194–3205

Ragni L, Nieminen K, Pacheco-Villalobos D, Sibout R, Schwechheimer C, Hardtke CS (2011) Mobile gibberellin directly stimulates Arabidopsis hypocotyl xylem expansion. Plant Cell **23**: 1322–1336

Ravichandran SJ, Linh NM, Scarpella E (2020) The canalization hypothesis - challenges and alternatives. New Phytol **227**: 1051–1059

Sander JD, Maeder ML, Reyon D, Voytas DF, Joung JK, Dobbs D (2010) ZiFiT (Zinc Finger Targeter): an updated zinc finger engineering tool. Nucleic Acids Res **38**: W462–468

Sang X, Li Y, Luo Z, Ren D, Fang L, Wang N, Zhao F, Ling Y, Yang Z, Liu Y, et al. (2012) CHIMERIC FLORAL ORGANS1, encoding a monocot-specific MADS box protein, regulates floral organ identity in rice. Plant Physiol **160**: 788–807

Sauer M, Balla J, Luschnig C, Wisniewska J, Reinohl V, Friml J, Benkova E (2006) Canalization of auxin flow by Aux/IAA-ARF-dependent feedback regulation of PIN polarity. Genes Dev **20**: 2902–2911

Schrader J, Baba K, May ST, Palme K, Bennett M, Bhalerao RP, Sandberg G (2003) Polar auxin transport in the wood-forming

tissues of hybrid aspen is under simultaneous control of developmental and environmental signals. Proc Natl Acad Sci USA **100**: 10096–10101

Sehr EM, Agusti J, Lehner R, Farmer EE, Schwarz M, Greb T (2010) Analysis of secondary growth in the Arabidopsis shoot reveals a positive role of jasmonate signalling in cambium formation. Plant J **63**: 811–822

Smetana O, Makila R, Lyu M, Amiryousefi A, Sanchez Rodriguez F, Wu MF, Sole-Gil A, Leal Gavarron M, Siligato R, Miyashima S, et al. (2019) High levels of auxin signalling define the stem-cell organizer of the vascular cambium. Nature **565**: 485–489

Suer S, Agusti J, Sanchez P, Schwarz M, Greb T (2011) WOX4 imparts auxin responsiveness to cambium cells in Arabidopsis. Plant Cell **23**: 3247–3259

Sun TP (2010) Gibberellin-GID1-DELLA: a pivotal regulatory module for plant growth and development. Plant Physiol **154**: 567–570

Sundberg B, Uggla C, Tuominen H (2000) Cambial growth and auxin gradients. *In* R Savidge, J Barnett, R Napier, eds, Cell and Molecular Biology of Wood Formation. BIOS Scientific Publishers, Oxford, pp 169–188

Sundell D, Street NR, Kumar M, Mellerowicz EJ, Kucukoglu M, Johnsson C, Kumar V, Mannapperuma C, Delhomme N, Nilsson O, et al. (2017) AspWood: high-spatial-resolution transcriptome profiles reveal uncharacterized modularity of wood formation in *Populus tremula*. Plant Cell **29**: 1585

Tuominen H, Puech L, Fink S, Sundberg B (1997) A radial concentration gradient of indole-3-acetic acid is related to secondary xylem development in hybrid aspen. Plant Physiol **115**: 577–585

Uggla C, Mellerowicz EJ, Sundberg B (1998) Indole-3-acetic acid controls cambial growth in scots pine by positional signaling. Plant Physiol **117**: 113–121

Uggla C, Moritz T, Sandberg G, Sundberg B (1996) Auxin as a positional signal in pattern formation in plants. Proc Natl Acad Sci USA **93**: 9282–9286

Ulmasov T, Liu ZB, Hagen G, Guilfoyle TJ (1995) Composite structure of auxin response elements. Plant Cell **7**: 1611–1623

Vanneste S, Friml J (2009) Auxin: a trigger for change in plant development. Cell **136**: 1005–1016

Vernoux T, Brunoud G, Farcot E, Morin V, Van den Daele H, Legrand J, Oliva M, Das P, Larrieu A, Wells D, et al. (2011) The auxin signalling network translates dynamic input into robust patterning at the shoot apex. Mol Syst Biol **7**: 508

Wang LJ, Ran LY, Hou YS, Tian QY, Li CF, Liu R, Fan D, Luo KM (2017) The transcription factor MYB115 contributes to the regulation of proanthocyanidin biosynthesis and enhances fungal resistance in poplar. New Phytol **215**: 351–367

Wareing PF (1964) University courses in biology. Nature **202**: 1064

Wenzel CL, Schuetz M, Yu Q, Mattsson J (2007) Dynamics of MONOPTEROS and PIN-FORMED1 expression during leaf vein pattern formation in *Arabidopsis thaliana*. Plant J **49**: 387–398

Xu C, Shen Y, He F, Fu X, Yu H, Lu W, Li Y, Li C, Fan D, Wang HC, et al. (2019) Auxin-mediated Aux/IAA-ARF-HB signaling cascade regulates secondary xylem development in Populus. New Phytol **222**: 752–767

Yang H, Han Z, Cao Y, Fan D, Li H, Mo H, Feng Y, Liu L, Wang Z, Yue Y, et al. (2012) A companion cell-dominant and developmentally regulated H3K4 demethylase controls flowering time in Arabidopsis via the repression of FLC expression. PLoS Genet **8**: e1002664

Yoshimoto K, Jikumaru Y, Kamiya Y, Kusano M, Consonni C, Panstruga R, Ohsumi Y, Shirasu K (2009) Autophagy negatively regulates cell death by controlling NPR1-dependent salicylic acid signaling during senescence and the innate immune response in Arabidopsis. Plant Cell **21**: 2914–2927

Zeng J, Zhang M, Hou L, Bai W, Yan X, Hou N, Wang H, Huang J, Zhao J, Pei Y (2019) Cytokinin inhibits cotton fiber initiation by disrupting PIN3a-mediated asymmetric accumulation of auxin in the ovule epidermis. J Exp Bot **70**: 3139–3151

Zhang J, Eswaran G, Alonso-Serra J, Kucukoglu M, Xiang J, Yang W, Elo A, Nieminen K, Damen T, Joung JG, et al. (2019) Transcriptional regulatory framework for vascular cambium development in Arabidopsis roots. Nat Plants **5**: 1033–1042